Small, fast and tough: shrinking down integrated elastomer transducers

Samuel Rosset[1, a)] and Herbert R. Shea[1]
École polytechnique fédérale de Lausanne, Neuchâtel, Switzerland

We review recent progress in miniaturized dielectric elastomer actuators, sensors and energy harvesters. We focus primarily on configurations where the large strain, high compliance, stretchability and high level of integration offered by dielectric elastomer transducers provide significant advantages over other mm or µm-scale transduction technologies. We first present the most active application areas, including: tunable optics, soft robotics, haptics, micro fluidics, biomedical devices and stretchable sensors. We then discuss the fabrication challenges related to miniaturization, such as thin membrane fabrication, precise patterning of compliant electrodes, and reliable batch fabrication of multilayer devices. We finally address the impact of miniaturization on strain, force and driving voltage, as well as the important effect of boundary conditions on the performance of mm-scale DEAs.

Keywords: soft actuators; dielectric elastomer actuators; miniaturization; scaling laws

I. INTRODUCTION

Soft and stretchable transducers are key elements in many areas including soft robotics[1–3], haptic devices for touch interaction with humans[4–7], tunable optics[8–11], energy harvesting[12–14], and microfluidics[15–17].

Compared to their rigid counterparts, soft actuators present many unique properties that enable a broad new range of applications. While systems based on traditional actuators work by moving rigid parts relative to each other, soft actuators can modulate their entire shape or change their stiffness locally. This provides distributed actuation and allows soft systems to adapt to their environment. Thus, soft actuators are able to perform tasks that would be difficult or impossible to achieve with electric motors and mechanical joints, or other rigid actuators[1–3]. In addition, actuation mechanisms taking advantage of the non-linear mechanical properties of soft materials lead to enhanced performance. For example, conventional air gap electrostatic actuators are limited to vertical strains of −33 % due to the electromechanical instability, whereas cleverly designed soft electrostatic actuators can exhibit up to 1692 % of area strain[18] (corresponding to −94.4 % thickness strain).

Different actuation methods drive soft actuators. Pneumatic actuation can be used to inflate deformable chambers in order to create distributed bending[1,3,19]. Fiber-reinforced expandable chambers can also produce uniaxial contraction when used in a McKibben configuration[20,21]. Electromechanically active polymers (EAPs), both in the form of ionic EAPs[22,23] and dielectric elastomer actuators (DEAs)[24–27] are also interesting candidates due to the direct conversion from electrical energy to mechanical deformation. Finally, shape memory polymers, or phase change materials can be used to produce large deformation by thermal activation[28–30].

We focus this review on Dielectric Elastomer Transducers (DETs)[24–27] (i.e. actuators, sensors, and generators), which combine high strains (up to 1692 % increase in surface[18]), high energy density[24] and no power consumption to hold a static position. In addition, they have a simple structure, as they are basically rubbery capacitors: a dielectric membrane sandwiched between two compliant electrodes[24]. In actuation mode, when a voltage is applied between the electrodes, the generated Maxwell stress causes the membrane to contract in thickness and to increase in surface[24]. Extensive reviews have been published on the subject[25], including on materials[36,37], electrodes[38,39], applications[26], and on the theory describing their behavior[40,41].

Most of the time, DETs are used as actuators: the applied electric field leads to a mechanical deformation. Actuators require driving fields of the order of 100 V µm^{-1} to 150 V µm^{-1}, which translates into actuation voltages between 1 kV and 15 kV for the typical membrane thicknesses. In the generator configuration, a mechanical deformation increases the energy of electrical charges placed on the device, leading to conversion of mechanical work into electrical energy. In addition to actuators and generators, DETs can also be used as soft and stretchable sensors, by measuring the change of capacitance induced by deformation. One of the advantages of sensors – compared to actuators and generators – is that they don't require high electric fields. This is particularly relevant in a context of miniaturization. If all dimensions of a device are scaled down, including the thickness of the dielectric membrane, then the production of membranes becomes a critical point (see section III A). Tiny defects such as inclusion of bubbles or thickness inhomogeneities are more critical on thin DETs, and often lead to premature breakdown when high electric fields are applied. Capacitive sensors can be probed with a much lower electric field than what an actuator requires, and they are consequently much more tolerant to defects in the dielectric.

DETs can also combine multiple functions. An actuator can be simultaneously used as sensor to measure its own deformation, a principle known as capacitive self-sensing[42,43]. Self-sensing enables to drive DEAs in close-loop mode, adapting the control voltage to keep the capacitance (and therefore the deformation) at a fixed set point. The generator and sensor functions can also be

a)Electronic mail: samuel.rosset@epfl.ch

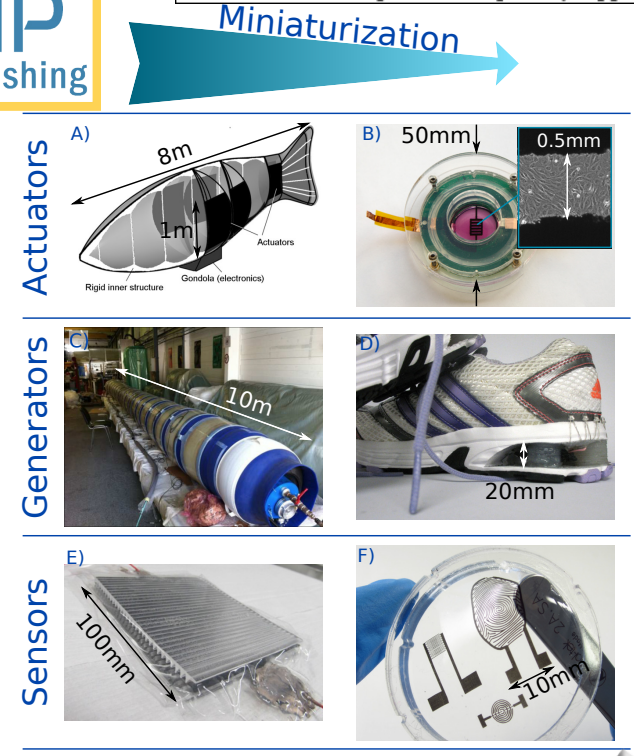

FIG. 1. Dielectric elastomers transducers at different size scales. Actuators: A) 8 m-long blimp with several square meters of actuators[31]. ©2010 SPIE. Reproduced with permission. B) Bio-reactor for the study of cellular mechanotransduction with electrode size in the mm range[32]. Generators: C) 10 m-long tubular wave energy converter prototype[12]. ©2012 SPIE. Courtesy of SBM Offshore and reproduced with permission. D) Soft generator integrated into the heel of a sneaker[33]. ©2012 Auckland Bioengineering Institute. Reproduced with permission. Sensors: E) 100 mm × 100 mm compression sensor[34]. ©2015 SPIE. Reproduced with permission. F) capacitive proximity sensors with interdigitated electrodes including features down to 100 µm[35].

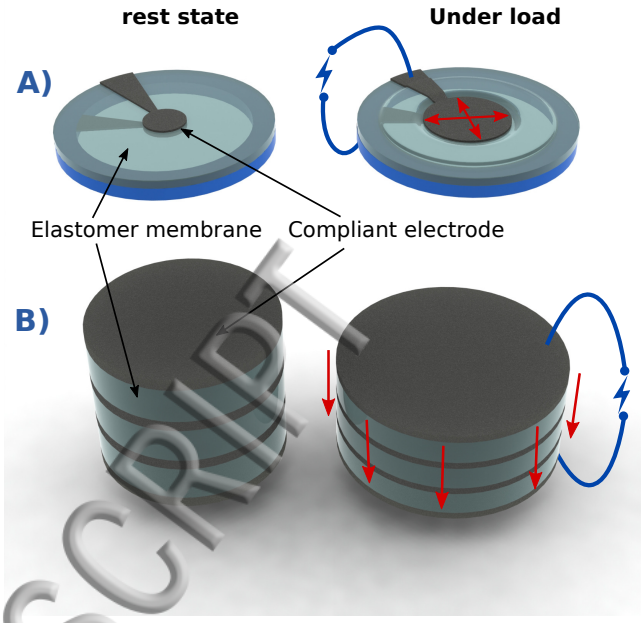

FIG. 2. A) Surface expansion DET: electrodes patterned on a prestretched membrane. B) Thickness compression DET: a stacked transducer composed of several electrode/elastomer layers. For actuators, an electrical energy input (blue bolt) leads to a mechanical deformation (red arrows). For generators or sensors, a mechanical deformation (red arrows) generates electrical energy or a change of capacitance (blue bolt).

combined in a single device, either to synchronize the harvesting cycle, or to obtain self-powered sensors[44].

DETs have been fabricated on size scales ranging from several square meters in the case of wave energy converters[12] or a biomimetic blimp[31], down to 1×10^{-2} mm^2 for miniaturized devices[45,46]. This difference in size scale among DETs is illustrated in figure 1, with examples for actuators, generators and sensors of different sizes. Although the 6 examples presented on the figure have active areas that differ by several orders of magnitude, the thickness of the dielectric membrane is similar for all of them.

Here, we concentrate on small-scale DETs made with scalable fabrication processes inspired by standard microfabrication techniques, and compatible with integration in complex systems. Miniaturized DETs possess a unique combination of characteristics compared to traditional microactuators, including large strains, short response time, high energy density, low power consumption, and resistance to shocks and extreme deformations. Fabrication techniques inspired by the world of microelectromechanical systems (MEMS) allow reproducible and reliable batch fabrication of devices, and enable the design of complex systems composed of many electrically independent actuators patterned on the same substrate, such as braille tactile displays[47] or arrays of microactuators to stretch biological cells[45].

The many different DET configurations can be split into two main categories depending on how the mechanical deformation of the elastomer is exploited. Surface expansion and thickness compression occur concurrently in every DET due to the volume invariance of elastomers. The two categories below differentiate which of the two phenomena is employed in a given application, and not which deformation modes occurs: both are always present.

- Surface expansion transducers (figure 2 A), which exploit the lateral expansion of the electrodes (i.e. the area strain). These transducers usually consist of a membrane prestretched on a rigid frame, which allows taking advantage of the non-linear properties of elastomers to suppress the electromechanical instability and reach very large defromations[41,48]. In a planar configuration, a surface strain up to 488 % has been observed[49], while a more complex diaphragm setup led to strains up to 1692 %[18].

Examples of devices relying on the surface expansion mode include diaphragm Braille tactile display[47], tunable gratings[10], deformable cell culture systems[45], or minimum energy structures[50].

- Thickness compression transducers (figure 2 B), which rely on the thickness compression of the membrane (i.e. thickness strain). These actuators are usually non prestretched and are therefore limited to a thickness strain of $-33\,\%$ due to electromechanical instability. Because the elastomer membrane thickness is typically $10\,\mu m$ to $100\,\mu m$, compression transducers are usually stacked on top of each other to increase the total height of the structure and obtain usable displacements. Applications of stacked compression transducers include haptic feedback interfaces[5], active vibration damping[51], energy harvesters[14] and valves[52].

In the next section (section II) we review the different application areas of small-scale DETs. We then discuss fabrication challenges related with the miniaturization of DETs (section III), before looking at what are the impacts of miniaturization on the performance of such transducers (section IV). Finally, we look at ways to combine DETs with other actuation method in order to increase the output force, while keeping the large strains that characterize DEAs (section V).

II. APPLICATION AREAS OF SMALL-SCALE DEAS

In this section, we review a few applications of miniaturized dielectric elastomer actuators. The smallest significant dimension of the patterned electrodes from the cited examples is comprised between $100\,\mu m$ and $25\,mm$.

A. Haptic interfaces

The sense of touch and tactile feedback have long been neglected in the interaction between machines and humans. Tactile displays are hard to the touch and flat, and they usually provide feedback to user-input acoustically. Although mobile devices usually have a vibrating alert, these devices work at a single fixed frequency and only generate binary sensory output, thus limiting the information that can be carried to the users.

The company Artificial Muscles Inc. (now part of Parker[53]) developed a haptic interface based on DEAs capable of generating vibration over a large frequency spectrum of about $200\,Hz$[4]. The device consists of an in-plane prestretched membrane, partially covered by electrodes. An inertial mass is placed on the passive part of the membrane and is set in motion by the area expansion of the electrodes. This concept has been used in two commercial products: a) an add-on case for iPod Touch aimed at providing gamers with realistic haptic feedback, such as a ball rolling on a wooden floor, hitting walls or falling into holes in the Maze game (figure 3), and b) headphones that transform the lower end of the musical spectrum (basses) into vibrations, thus providing "4D" sound experience. The actuator footprint is $76\,mm \times 36\,mm$ and contains several (4 to 7) small-size actuators patterned on the membrane[4].

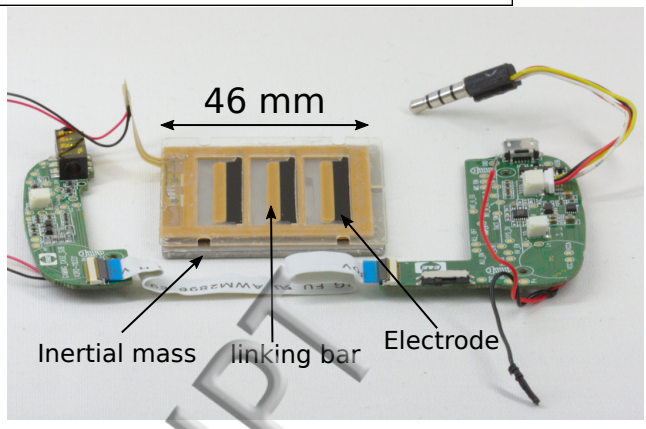

FIG. 3. Actuator and high voltage control electronics of the haptic interface for iPod Touch by Artificial Muscles Inc.The three transversal linking bars on the membrane are fixed to the inertial mass.

Another approach for a DEA-based tactile interface has been developed at TU Darmstadt, based on stacked compressive actuators[5,54,55]. The device consists of a totally soft portable media player control interface capable of detecting user input through capacitive self-sensing (c.f. section II G), and providing feedback to the user via vibrotactile feedback. The complete device is about $40\,mm$ in diameter and holds 5 electrically-independent DETs that integrate sensing and actuation capabilities (for the play/pause, stop, previous, next, and volume functions). The 5 stacked transducers are produced in parallel by an automated process that is discussed later (c.f. section III D).

Both devices are good illustrations of the miniaturization of DETs, as they include multiple independent transducers (actuators/sensors) on a single membrane with precisely patterned electrodes, and a production process – in the case of the AMI commercial devices – optimized for mass market production. The second notable point is that both applications are intended to be integrated into portable consumer products, and must consequently have the smallest possible footprint, including the driving electronics. Despite the high driving voltage required to drive DEAs, both applications managed to fit all the parts in a reduced volume. The "4D" sound system for headphone including controls fits alongside the audio components in a normal-size headphone set, whereas a demonstrator of the media player interface was assembled together with control electronics in a box of $150\,mm \times 80\,mm \times 20\,mm$[55].

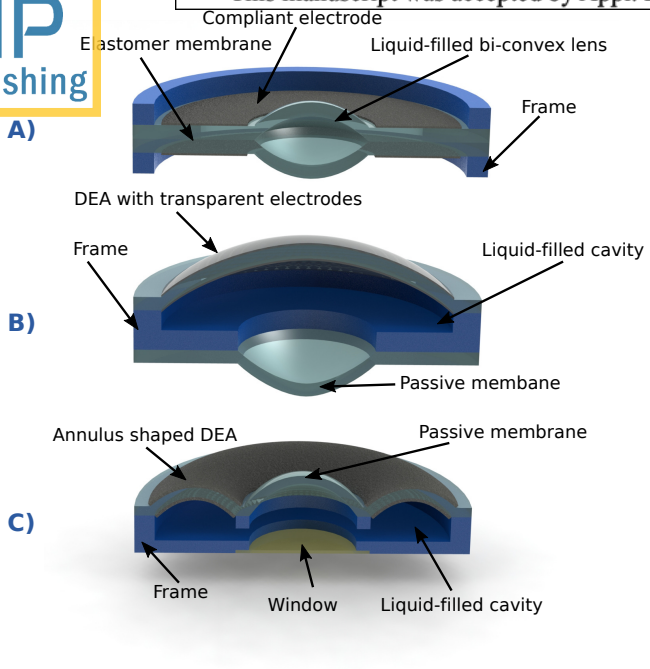

FIG. 4. 3 DEA-based tunable lens concepts. A) Bioinspired lens with two bonded elastomer membranes encapsulating a liquid at the center. Upon activation, the annulus-shaped electrodes expand and compress the lens, thus changing its radius of curvature[8]. B) A DEA membrane with transparent electrodes and a passive elastomer membrane are placed on opposite sides of a cavity filled with liquid. Upon activation of the DEA, the active membrane expands and the passive membrane relaxes, leading to a change of curvature of both membranes[9]. C) Similar concept than for B), but the actuator is located on the side, thus avoiding the need for transparent electrodes[56].

B. Tunable optics

The field of tunable optics has much to gain from miniaturized soft actuators. While conventional devices are based on rigid mechanical components that are moved relative to each other, soft actuators provide tuning through deformation. Conventional optical zooms are based on the translation of rigid lenses, often driven by electromagnetic or piezoelectric motors. They are limited in speed due to the inertia of the moving elements, can be noisy and quite bulky. In comparison, a soft lens can control its radius of curvature to change its focal length. Because there is no parts that need to translate, soft lenses are quite compact, operate silently and have short response times.

Different concepts of tunable lenses based on small-scale DEAs have been published. They are usually based on a high-refractive-index liquid encapsulated by a thin elastomer membrane that deforms upon actuation. This deformation leads to a change of curvature – and therefore of focal length – of the lens. Carpi et al. have developed a bio-inspired lens that consists of two elastomer membranes bonded together and encapsulating a small pocket of liquid at the center, thus forming a lens (figure 4 A)[8]. The annulus-shaped electrodes are applied around the lens. Upon activation, the actuator expands in-plane and compresses the lens. The focal length of the lens changes from 22.7 mm at rest down to 16.7 mm with an applied voltage of 3.5 kV, which represents a tuning range of −26.4 %. Because actuation causes a decrease of the radius of curvature of the lens, and given the proportionality between the focal length and the radius of curvature, the tuning range of this design is therefore fairly limited.

This issue is solved by the approach used by Shian et al. with their fluidically coupled lens[9]. It consists of two elastomer membranes of different diameters placed on opposite sides of a frame. A transparent liquid is injected in the device, filling the cavity and partially inflating the two membranes, the larger one being a DEA with transparent electrodes (figure 4 B). When a voltage is applied to the active membrane, it expands, which causes a reduction of the internal liquid pressure and deflates the passive membrane, whose radius of curvature increases, causing an increase of the focal length of the system. Using an active/passive membrane diameter ratio of 1.6, the authors were able to obtain a relative tuning range of 100 % at 5 kV, starting from an initial focal length of 36 mm[9]. Although the tuning range of this concept is about four time larger than the previous approach, it has the disadvantage of requiring the use of transparent compliant electrodes. The authors have used single walled carbon nano-tubes, but the impact of the two layers of electrodes on light transmission and scattering has not been quantified.

A third design from Wei et al. presents a large tuning range without the need for transparent electrodes. It uses the same principle than of fluidically coupled membranes from the previous example, but instead of mounting the membranes back to back, they are positioned on the same plane, with the actuator having an annulus shape around the passive lens (figure 4 C)[56]. In theory, it should be possible to completely suppress the internal fluid pressure by activating the DEA, leading to a completely flat lens and to an infinite focal length. With their device, the authors were able to obtain a relative tuning range of 300 % for a 1 kV actuation voltage.

An alternative solution to the requirement for electrodes that do not absorb nor scatter light has been proposed by Keplinger et al. with their electrode-free approach. Using a design similar to the lens of figure 4 A, but without electrodes, the authors have sprayed opposite charges on each side of the lens. The electrostatic force causes an attraction of the two membranes defining the lens against each other, thus leading to an increase of the radius of curvature[57].

Alongside lenses based on the deformation of a thin elastomer membrane, other concepts have been proposed, for example using DEAs to modify the curvature of the meniscus between two liquids[58], or between a liquid and

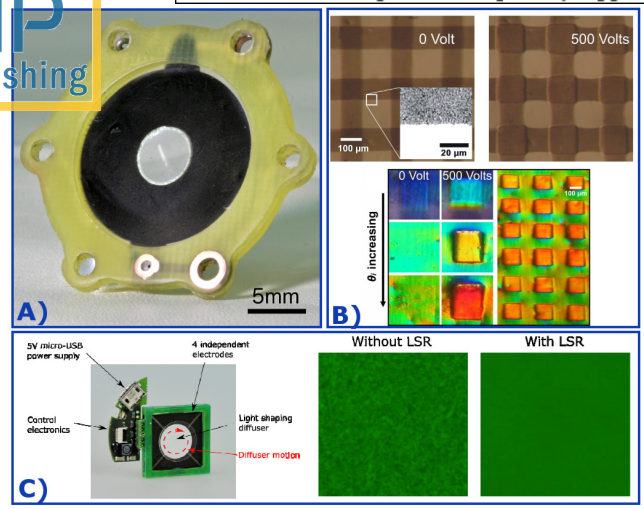

FIG. 5. DEAs applied to optical components. A) Soft tunable lens made with two silicone membranes bonded together and encapsulating a transparent liquid at the center (concept shown on figure 4 A)[70]. B) Reflective tunable grating with an array of 100 µm × 100 µm electrodes[46]. ©2007 SPIE. Reproduced with permission. C) Left: Optotune's Laser speckle reducer LSR-10-22 with a diameter 10 mm clear aperture and control electronics. Right: speckle contrast of a laser beam on a screen with and without a Laser speckle reducer[67]. ©2015 SPIE. Reproduced with permission.

air[59], with sub-mm lenses demonstrated in the latter case[59].

In addition to lenses (figure 5 A), other tunable optical components based on DEAs have been developed. DEA-based tunable gratings use the in-plane expansion of the electrodes to deform a soft grating placed on the surface of the membrane(figure 5 B)[10,46,60–64]. Thanks to the large actuation strain of DEAs, more than 30 % change in grating period has been obtained[64,65]. The Swiss company Optotune[66] has commercialized a DEA-based device to reduce the contrast of speckles in Laser-based projection systems[67]. The device consists of a diffuser placed at the center of a prestretched membrane, with 4 electrically-independent electrodes located around it. The electrodes are successively activated to move the diffuser along a circular path, thus destroying the spatial and temporal coherence of the laser beam (figure (5 C)). The electrodes are driven at the in-plane mechanical resonance frequency of the membrane (300 Hz) to maximize the motion and the reduction of the speckle contrast. In its version with a diameter 5 mm diffuser, the device measures 17 mm × 17 mm × 3.8 mm and weighs 2.5 g including the control electronics. Other examples of soft optical devices based on DETs include a tunable phase shifter[68] and tunable photonic crystals elastomers[69].

The applications that require tuneable optical component usually benefit from the extended tuning range or compactness offered by DEAs. However, they also often require the actuator to be able to quickly shift from one configuration to the other, and then to stabilize at the target position. However, most of the DEA-based optical devices mentioned above are made with an acrylic elastomer named VHB[8–10,46,60–63,68], which suffers from high mechanical losses. This leads to slow response time and viscoelastic creep[71,72], two undesirable properties for optical applications. Silicone elastomers are also widely used to make DEAs, and have a much lower mechanical loss factor than VHB. They are therefore more suitable than VHB for optical applications. But because they are generally stiffer, they generate less strain, and thus VHB is often preferred for scientific publications.

A recent study from Maffli et al. comparing the performance of the biomimetic lens design from[8] has shown that the response speed of a silicone-based lens was up to 3 orders of magnitude faster than a similar lens made with VHB[70]. With a settling time of 175 µs, the soft silicone-based lens exhibits an extremely fast response, thanks to the small amount of liquid that needs to be displaced to change the focal length. The same article also presents a process flow for the reliable fabrication of lenses with silicone membranes, patterned electrodes, and liquid encapsulation[70].

Drift due to viscoelastic creep in the membrane makes it difficult for a DEA to hold a static position. But capacitive self-sensing can be used to drive an actuator in closed-loop mode to hold a stable position and suppress drift (c.f. section II G). A study from Rosset et al. on tunable gratings driven in closed loop and relying on the measurement of the device capacitance has shown that silicone membranes were more suitable than VHB for maintaining a completely stable position[62].

C. Soft robotics

Being soft by nature, DEAs are ideal actuators for soft robots. Pneumatic actuation is common in the field[1,3], but requires many external components (fluid transmission lines, valves, pumps, etc.) that can be much more voluminous than the device itself (see e.g. figure 3 from reference[3]). With DEAs, the actuator can be integrated in the robot itself, leading to more compact and independent soft robots. The control electronic can also be mounted on the robot, eliminating the need for tethering to outside components.

One illustration of this concept is the foldable elevons from Shintake et al. that are used as control surfaces of a micro air vehicle (MAV) (figure 6)[50]. The propeller, the foldable DEAs for attitude control, the electronics and the batteries are mounted on a 400 mm wingspan remote-controlled MAV capable of flying and maneuvering. The actuators used for the MAV elevons are based on dielectric elastomer minimum energy structures (DEMES), a concept introduced by Kofod et al. and that consists in fixing a prestretched DEA to a flexible (but not stretchable) frame. The partial relaxation of the membrane leads to complex 3D structures whose shape can be controlled by voltage[73]. DEMES have been used for soft

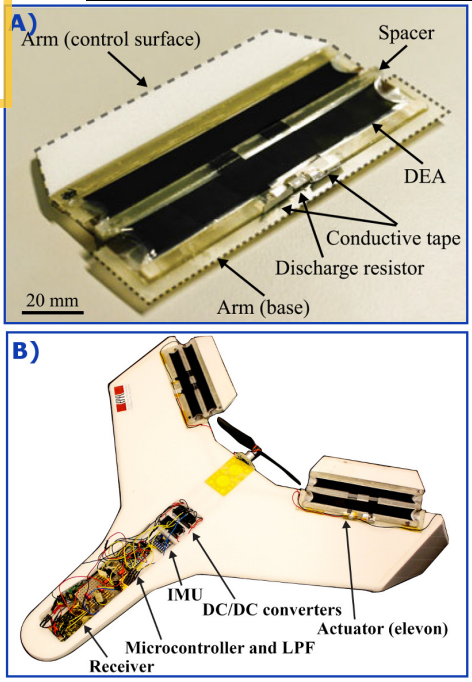

FIG. 6. A) Elevon actuators used as control surface for a micro air vehicle (MAV). The actuator can bend up to 25° when activated, and provides a torque up to 2750 mN mm. B) Two elevon actuators are mounted on a MAV frame with a 400 mm wingspan, together with a propeller, battery, and all the necessary control components, for a total mass of 130.7 g. The prototype and its ability to be controlled by the DEA-elevons has been demonstrated during a 150 s flight that included a arm-throw take-off and ground landing[50]. ©2015 IEEE. Reproduced with permission.

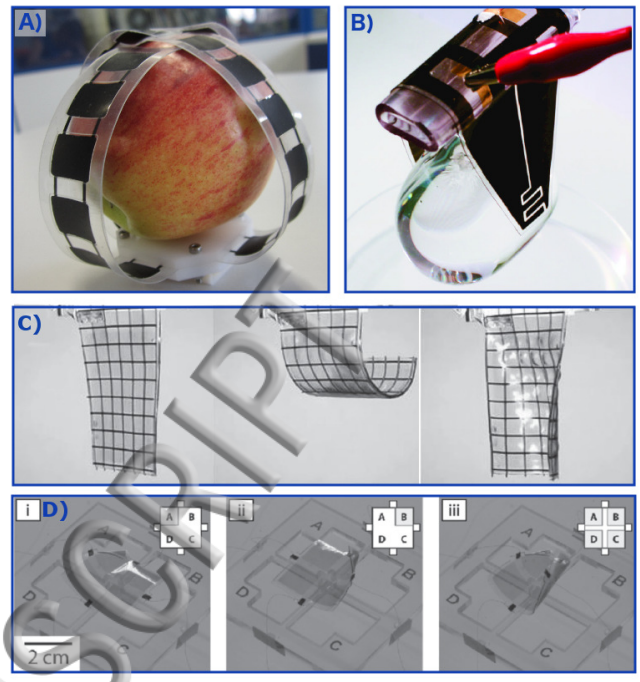

FIG. 7. A) Rollable multi-segment DEMES in a four-finger configuration[75]. ©2015 IEEE. Reproduced with permission. B) soft gripper combining DEA actuation for grasping objects, and electroadhesion to hold them. The ability of soft grippers to conform to the shape of the target allows to handle all kind of objects, in that case a thin silicone membrane filled with water[2]. ©2016 WILEY-VCH Verlag GmbH. Reproduced with permission. C) Soft DEA gripper using stiff fibers to produce folding motion that conforms to object. Using a dual actuator configuration with fibers oriented perpendicularly on each side of the device allows obtaining vertical or horizontal bending, depending on which actuator is activated[76]. ©2016 WILEY-VCH Verlag GmbH. Reproduced with permission. D) Multilayer multimorph actuator based on spin-coated acrylic elastomer layers and capable of 9 different configurations. i) Top left corner activated. ii) Top right corner activated. iii) All four electrodes activated[77]. ©2016 WILEY-VCH Verlag GmbH. Reproduced with permission.

robotic applications by different authors, such as a 3 fingers gripper from Kofod et al.[73], a multi-segmented robot capable of inchworm-like motion by Petralia and Wood[74], or a rollable multi-segment DEMES which has been developed as an end effector for a space debris removal system by Araromi et al.(figure 7 A)[75]

The ability of soft DEAs to conform to all kind of shapes makes them particularly suitable as micro-manipulators. Indeed, humans use their hands to pick up a large range of objects, varying in shape, weight and texture, whereas robotic manipulators are often optimized to handle a very specific target. But soft actuators, such as DEAs, can be used to design versatile grippers. Shintake et al. have recently shown how a clever electrode design enables combining DEA actuation with electroadhesion, the latter effect relying on the fringing field between interdigitated electrodes. They have applied the concept to a soft gripper that combines DEA actuation for the open-close motion with electroadhesion to conform to the shape of the target and provide the holding force (figure 7 B)[2]. The gripper is able to pick up objects that differ widely by their shape and structure, such as a flat piece of paper, a chicken egg, a Teflon cylinder, a very thin water-filled silicone balloon that changes shape while it is being picked up, etc. The device weighs 1.5 g and was able to pick up and hold objects up to 82.1 g. The authors have shown that an optimal design of the interdigitated electrodes – that are used both for the DEA bending actuation and for the electroadhesion – allows obtaining large shear forces (up to 3.5 N), while still keeping a large enough area coverage for DEA actuation (23° bending angle, versus 30° for non-interdigitated electrodes)[2].

Another approach to a DEA-based soft gripper that can conform to the shape of various objects has been proposed by Shian et al. It consists of a non-prestretched sheet of acrylic elastomer reinforced with stiff fibers (figure 7 C)[76]. Depending on the density and orientation of the fibers, the sheet of elastomer exhibit different bending configurations when a voltage is applied between the

This manuscript was accepted by Appl. Phys. Rev. Click here to see the version of record.

electrodes. Duduta et al. have used a similar concept to produce a bending actuator based on a non-prestretched acrylic elastomer membrane[77]. Rather than using a commercial acrylic elastomer film, they have spin-coated UV curable layers to a thickness of around 25 µm, leading to an actuation voltage of 1 kV to 2 kV, i.e. much less than the >5 kV required for the actuators from Shian et al.[76]. To compensate for the loss of force induced by the thinner dielectric layers, Duduta et al. have produced multilayer structures with up to 7 layers. Attempts to further decrease the elastomer thickness have yielded actuation voltages down to 600 V. However, the results were not reproducible due to a lower yield caused by the inclusion of airborne particles[77]. The fabrication of layer-by-layer stacked actuators is discussed in more details in section III D. Duduta et al. have used a layout with 4 independent electrodes, allowing to activate each corner of the actuator separately (figure 7 D), thus effectively creating a multimorph with 9 different configurations.

D. Biomedical applications

Miniaturized DETs are of great interest for deformable cell culture assays used in mechanotransduction studies. Indeed, standard static in vitro cell cultures are not truly representative of the conditions cells are submitted to in the body, where they are constantly strained and submitted to mechanical stress. Periodically stretching cells in vitro allows monitoring the effects of strain, such as gene expression, change of morphology, or differentiation. Commercial cell-stretching systems exist, such as Flexcell's FX-5000T[78], but they have limitations: the whole cell culture is stretched with the same equi-biaxial strain, and the pneumatic actuation requires bulky equipment next to the culture wells.

DEA-based deformable cell culture systems solve the shortcomings of traditional equipment and bring new interesting features. Patterned electrodes on a small size scale form arrays of independent actuators on a single membrane. This configuration enables stretching small cell populations (or even single cells) instead of the complete culture. The actuators being electrically independent, each can be driven at different strains and/or frequencies, thus enabling high throughput experiments on a single cell culture. Akbari et al. have presented an array of 100 µm × 100 µm cell-stretching actuators exhibiting up to 80 % strain[45,79]. Unlike the Flexcell device, Akbari's actuators produce uniaxial strain, which is more relevant for mechanotransduction studies, because closer to the solicitation of cells in the body. But more importantly, DEAs can easily be designed to produce different types of strains. Poulin et al. have for example presented a device capable of compressing a small cell population up to −12.5 %[80].

The high electric field required to drive DEAs (up to 150 V µm^{-1}) is an obstacle to their application for deformable cell culture systems. First, it is important that the zone on which the cells are cultured remains free from electric field. Second, these devices must operate while immersed in conductive cell culture media. Poulin et al. have minimized stray electric field by having overlapping electrodes over the complete device. Additionally, it is also important to ensure that the conductive media doesn't act as a blanket electrode that would create a large amount of fringing field. The authors present different designs that prevent the cells from seeing large electric fields[81]. They also demonstrate long term actuation of a device immersed in a conductive media without failure (>45 kcycles). Poulin et al. have used their deformable bioreactor to periodically stretch lymphatic endothelial cells from 0 % to 10 % at 0.1 Hz for 24 h[32]. They show that cells submitted to the periodic strain align and elongate in a direction perpendicular to the stretching direction, while cells cultured outside of the stretching zone remain randomly oriented. Furthermore, a controlled experiment conducted on an immobilized device showed no alignment in the active zone, thus proving that the observed phenomena are due to the mechanical stretching and not to the fringing electric field[32].

Other biomedical applications based on small-scale DEAs have been developed or proposed, such as implantable artificial sphincters[82] and implantable artificial facial muscles. For example, Senders et al. have developed a DEA-based eyelid sling that was implanted in human cadavers and was able to make them blink[83]. The study was then extended to live gerbils on which the device was implanted[84]. The DEAs were actuated continuously with 1 kV at 1 Hz. The devices worked on average for 30.3 days, which represents 2.6×10^6 actuation cycles, and failure was attributed to electrical wire connection issues, rather than a failure of the actuator itself[84]. The animals were euthanized at the end of the test to conduct histologic analyses that showed minimal chronic inflammation. This study shows that despite the high actuation voltage, carefully designed miniaturized DEAs can be implanted and activated inside a living animal.

E. Microfluidics

The field of microfluidics is known for its multifunctional platforms that combine multiple assays on a single chip, such as labs-on-a-chip (LOC), micro total analysis systems (MicroTAS), and microfluidic large scale integrated systems (MLSI). Although the devices themselves can be densely integrated to pack a maximum of functions on a small footprint, they often rely on voluminous external components. For example, MLSI chips usually consist of an array of pneumatic actuators that can be used as pumps or valves[85]. They require external tubing, pneumatic switches and pressure sources to function. DEAs can be used in microfluidic applications to provide actuation where needed, removing the need for external tubing and pressure sources.

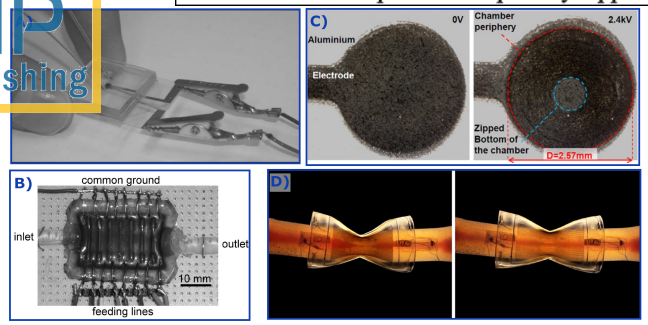

FIG. 8. A) DEA-powered all-polymer micropump[86]. ©2006 The Royal Society of Chemistry. Reproduced with permission. B) Peristaltic pump based on stacked DEAs. From[87]. ©2009 SPIE. Reproduced with permission. C) Zipping dielectric elastomer actuator closing a conical cavity. Left: at 0 V the membrane is suspended over the cavity. Right: at 2.4 kV the membrane zips down the cavity until it reaches the bottom[17]. ©2013 IOP publishing. Reproduced with permission. All rights reserved. D) Dielectric elastomer valve around a silicone tube. Left: at 0 V, the valve squeezes the tube and creates resistance to the flow of liquid. Right: at 3.2 kV the valve is open and does not alter the flow[88]. ©2015 IOP publishing. Reproduced with permission. All rights reserved.

Loverich et al. have developed a micropump that consists of two membranes coupled by a fluid, one of them being a DEA, as well as passive PDMS valves. When driven with 3.3 kV at 30 Hz, the pump exhibits a flow rate of 77.4 µl min^{-1} for a total footprint under 10 mm^2 (figure 8 B)[86]. Lotz et al. have demonstrated a peristaltic pump made from multilayer stacked actuators produced with an automated process that is discussed in more details in section III D[87]. The pump exhibits a flow rate of 0.36 µl min^{-1} on a footprint of 40 mm × 55 mm (figure 8 B).

McCoul and Pei report on a tubular dielectric elastomer valve capable of squeezing a soft silicone tube passing through it[88]. When a flow of 200 ml h^{-1} is forced through the tube by a syringe pump, the valve can control the pressure in the system, from 3.3 kPa at 0 V (the valve pinches the tube) down to 0 Pa at 2.4 kV (the valve is open and does not restrict the flow in the tube) (figure 8 D).

Maffli et al. have proposed the use of electrostatic zipping to close a micromachined chamber with a soft elastomer membrane, as a way to provide integrated actuation for MLSI chips[17]. Unlike typical DEAs with electrodes on both sides of the membrane, zipping actuators use a single electrode on the dielectric membrane; the cavity above which the membrane is suspended acting as the second electrode. The electrostatic force generated when a voltage is applied attracts the membrane into the cavity, sticking (i.e. zipping) the elastomer against the walls of the chamber, thus effectively closing it (figure 8 C). This concept allows making valves, and even peristaltic pumps if several units are placed in series and actuated with a phase shift[17].

F. Energy harvesting

Harvesting electrical energy from human motion has many potential applications, such as powering personal electronic equipment, or health monitoring devices. Different systems have been developed based on electromagnetic generators, such as backpacks that oscillate up and down, knee braces, and heel strike generators. However, these approaches are often bulky, noisy and obtrusive for the user. Piezoelectric generators have been used in shoe heels and backpacks to reduce obtrusiveness at the cost of a much lower energy density.

Human body motion is characterized by large amplitude movements at a low frequency (about 1 Hz for a person walking). This makes dielectric elastomer generators (DEGs)[12–14,89,90] particularly interesting for this task, as they can sustain large deformation and work well at low frequencies– unlike piezoelectric generators which work best at resonance and are limited to low strains.

DEGs combine high energy density (up to 0.3 J g^{-1})[90], noiseless operation and mechanical properties that makes them particularly suitable for integration into a shoe. SRI international developed the first DEG installed in a heel, made with a stack of 20 layers of VHB and capable of generating 0.8 J/step[90]. More recently McKay et al. have presented a miniaturized diameter 11 mm DEG based on stacked silicone membranes of 65 µm[14]. Two versions were assembled, with 48 and 128 layers, capable of generating 2.1 mW cm^{-3} and 3.8 mW cm^{-3}, taking the volume of passive end caps into account. This concept has been implemented into the sole of a shoe, and the generated energy used to light up LEDs[91].

DEGs can harvest energy using different types of cycles. In most cases, some charges are placed at a defined voltage on the DEG when it is stretched, and harvested at a higher voltage in the relaxed state[14]. In other words, it is necessary to spend energy at the beginning of each cycle in order to collect more energy. Consequently, The electronic circuitry which converts the charges harvested at high-voltage to a usable low voltage must be energy efficient, so that the collected energy after transformation is higher than the priming energy required for each cycle.

G. Sensing applications

When a DET structure is mechanically deformed, its capacitance changes. DETs can therefore also act as soft sensors capable of measuring large deformations. Although the principle is similar to the generator (an external mechanical deformation generates a change in electrical signal), sensors can work at low electric field and are therefore much easier to implement. For the same reason, they are also much less sensitive to defects in the

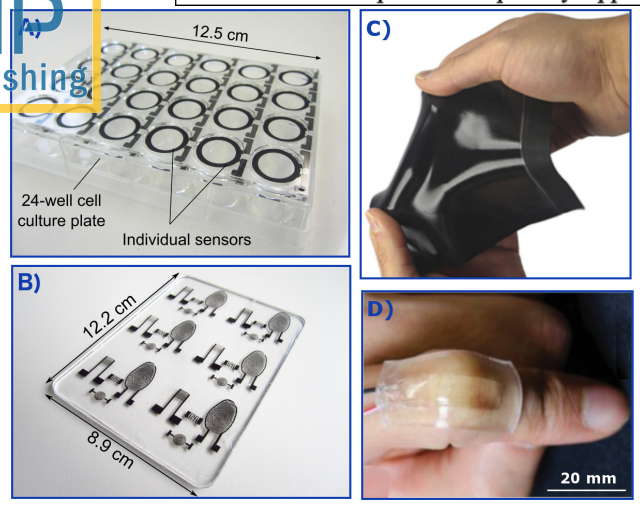

FIG. 9. A) Array of capacitive sensors mounted on a 24-well plate for detection of smooth muscle cells contraction[92]. ©2016 Elsevier Ltd. Reprinted with permission. B) Interdigitated proximity sensors patterned on PDMS by laser ablation. The technology allows to realize fine structures (down to 100 µm) over a large area[35]. ©2015 American Chemical Society. Reprinted with permission. C) 2D stretchable touch sensor with plain electrodes that relies on the transmission line characteristics of the electrodes[93]. ©2015 IOP publishing. Reproduced with permission. All rights reserved. D) Ionic skin with transparent hydrogel electrodes capable to sense deformation and pressure[94]. ©2014. WILEY-VCH Verlag GmbH. Reproduced with permission.

dielectric (see section III A), which makes it possible to have sensors made on ultra-thin membranes.

For example, Araromi et al. have made capacitive sensors with 5 µm thick PDMS membranes to measure the contraction of smooth muscle cells[95]. These very thin membranes are prestretched on a frame, with a pair of annular electrodes patterned on both sides (figure 9 A). Smooth muscle cells are located at the center of the device, and their contraction induces the stretching of the electroded area, thus leading to an increase of capacitance[92]. The device works in cell culture conditions with a mean standard deviation of 0.2 pF (0.05 % of the device initial capacitance), which makes it sensitive enough to detect the contraction of smooth muscle cells. Electrical detection of cell contractile strain enables continuous monitoring of many culture wells in parallel for high throughput experiments, which is not possible with conventional technique relying on optical observation.

The use of precise fabrication techniques allows patterning compliant electrodes on a very small scale. Araromi et al. have presented a sensor fabrication technique based on Laser ablation and oxygen plasma bonding to structure very fine (line width down to 100 µm) interdigitated electrodes (IDE) on silicone membranes (figure 9 B)[35]. These structures enable touch and proximity detection, relying on a change of capacitance induced by perturbation of the fringing field between the IDEs when a user approaches a finger. Unlike the parallel plate capacitor sensor that is exclusively sensitive to deformation, these IDE sensors are quite insensitive to stretch and can easily differentiate touch from a strain of up to 50 %[35]. They therefore keep their functionality even when deformed. The versatility of the fabrication method is demonstrated by fabricating an IDE touch sensor nested in the ground electrode of a DEA. A touch from the user on the sensor toggles pulsations of the actuator[96]. The sensitivity of the sensor is not affected by the high electric field of the actuator[35].

Small-scale patterning of electrodes enables the fabrication of an array of independent sensors to form a 2D sensitive surface. However, such a device requires many electrical connections ($n + m$ for a $n \times m$ matrix if a row/column addressing scheme is used), together with complex electronics. To solve this issue, Xu et al. have fabricated a 2D soft and stretchable keyboard using plain (i.e. unpatterned) electrodes (figure 9 C)[93,97]. The device relies on the relative poor conductivity of the carbon black electrodes to treat them as 2D transmission lines. Different signal frequencies are used to measure the capacitance of the device, with the lower frequencies probing the whole device, while the higher frequencies only probe the zone close to the electrical connection due to the low pass filter effect induced by the electrodes. The concept is demonstrated by measuring the capacitance of the device with two different frequencies (1 kHz and 60 kHz) in two orthogonal directions, effectively leading to a 2×2 (i.e. 4 sensitive zones) resolution. The concept was then scaled up to a 3×3 resolution simply by adding a third sensing frequency (20 kHz), and without any modification to the sensor itself or its electrical connections[93].

Sun et al. have developed a ionic skin capable of measuring stretching and pressure, based on a DET structure and capacitive sensing (figure 9 D)[94]. They use hydrogel electrodes made with a polyacrylamide gel and a NaCl solution as electrolyte. These electrodes are therefore completely transparent, and the whole device – consisting of an acrylic elastomer sandwiched between two hydrogel electrodes and encapsulated with additional acrylic elastomer layers – can be uniaxially stretched up to 6 times its original length[94].

The DET configuration (dielectric membrane sandwiched between two actuators) is not limited to actuators *or* sensors: the same structure can be simultaneously used as actuator *and* sensor, which enables driving actuators in closed-loop mode, without the need for an external sensor. This self-sensing approach allows suppressing drift caused by the viscoelastic creep of the elastomer, or rejecting external perturbations[43,62]. Gisby et al. have developed an algorithm to extract the capacitance (and other parameters) of DEA driven by a high voltage DC signal, to which a small AC signal is added[42].

III. FABRICATION OF SMALL SIZE DEVICES

A. Membrane processing

One of the advantage of scaling down DEAs is the reduction of the driving voltage, if we also consider decreasing the membrane thickness. Indeed, as a first approximation, the thickness strain s_z of a DEA can be described by[24]:

$$s_z = -\frac{\epsilon E^2}{Y} = -\frac{\epsilon V^2}{Y t^2}, \quad (1)$$

where ϵ is the permittivity of the dielectric, E the electric field, Y the Young modulus, V the applied voltage, and t the thickness of the membrane. Therefore, scaling down the membrane thickness also decreases the voltage required to reach a defined strain by the same factor. This is particularly important because DEAs usually work at fields from 100 V µm^{-1} to 150 V µm^{-1}, leading to actuation voltages of several kV when membranes with thicknesses from 10 µm to 100 µm are used. Membranes a few micrometers thick enable reducing the driving voltage to a few hundred volts, thus drastically simplifying the driving electronics and decreasing its footprint and cost.

The majority of DETs reported in the literature are based on a clear polyacrylate adhesive film from 3M named VHB, either VHB 4910 (thickness 1 mm) or VHB 4905 (thickness 500 µm), most of the time prestretched up to 25 times its initial area. This material is therefore too thick, even after prestretch, to be considered for very thin membranes. Silicones are the second largest group of elastomers used to manufacture DETs[36]. They are usually sold as liquid precursors, which enables the fabrication of layers of different thicknesses. Unlike pre-made films, custom-made membranes allow choosing independently the thickness of the layer and its prestretch, thus giving additional design freedom[98]. In addition, it gives the possibility to manufacture very thin membranes for low-voltage applications.

Silicone membranes can be made by different techniques, such as blade casting or spin-coating. In one of the first publications about DETs, Pelrine et al. report on the fabrication and release of silicone films down to 1 µm[99]. However, there is no indication on whether these membranes were used to make working actuators. Indeed, using ultra-thin membranes to make DEAs creates two important challenges: 1) the higher density of defects and 2) the patterning of the electrodes.

The first effect is caused by the unavoidable thickness inhomogenetity induced by the deposition technique, or the inclusion of bubbles and contaminants such as dust (figure 10). For thin membranes, this can lead to local weak zones where the electric field can be notably higher than on the rest of the membrane, and where dielectric breakdown is likely to occur. If the thickness inhomogeneity of the membrane deposition method is ± 1 µm, the electric field is 5 % higher at the thinnest location

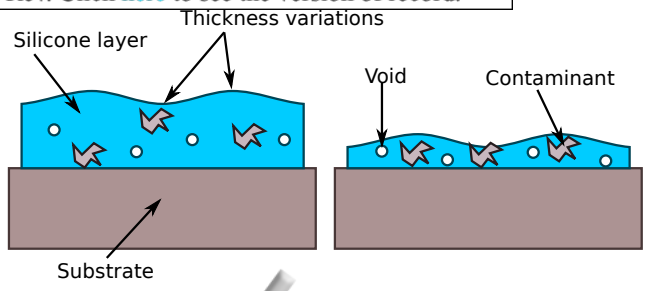

FIG. 10. Membranes can have thickness inhomogeneities, voids and air bubbles, or contaminants such as dust. Thick membranes (left) are less sensitive to these issues than thin membranes (right), for which defects can create zones of high electric field.

of a 20 µm membrane compared to the average value. If the membrane is only 5 µm, then the electric field can locally be up to 25 % higher than the average value. Similarly, contaminants and voids locally weaken the membrane, with a larger effect on thinner membranes, as the size of the defects or particles do not scale down with membrane thickness. Consequently, thinner membranes usually have a lower dielectric strength due to defects, thus reducing the maximal strain of the actuator. It is consequently important to select a membrane fabrication method that allows to deposit very homogenous layers without inclusion of bubble or voids, and to work in a controlled environment to prevent dust from contaminating the membrane.

Different methods have been proposed and demonstrated to make DETs based on very thin-membranes. Poulin et al. have fabricated 3 µm thick membranes by pad-printing[100]. They have used this technique to make and characterize expanding circles actuators and have obtained lateral strains of 7.5 % with only 245 V, i.e. about 1 order of magnitude less than a similar actuator with a 30 µm membrane. However, the maximal strain of the thinner actuator (7.5 %) is about half as much as the thicker one (14.2 %), due to a lower dielectric strength[100].

Töpper et al. have used molecular beam deposition to produce polydimethylsioxane films with thicknesses from 100 nm to 500 nm[101]. They have deposited 200 nm PDMS layers on thin PEEK foils to make bending actuators. The device exhibits a radius of curvature of 0.7 m for an actuation voltage of 12 V. A similar actuator made with a 4 µm thick spin-coated layer required a voltage 35 times larger to reach the same bending[101]. However, the thicker actuator was able to sustain an electric field twice as large than the sample made with molecular beam deposition.

Finally, Weiss et al. have used electrospraying to deposit PDMS layers in the hundreds of nanometers range[102]. They obtain films with surface roughness between 0.2 nm and 0.28 nm after UV curing, which is about 3 times lower than for a 2 µm film made by spin coating[102]. The authors have not yet applied this membrane fabrication technique to make fully functional

This manuscript was accepted by Appl. Phys. Rev. Click here to see the version of record.

DEAs, but it appears to be a promising technique, with a faster deposition rate compared to molecular beam deposition ($5.5\,\mathrm{nm\,s^{-1}}$ versus $130\,\mathrm{nm\,h^{-1}}$ for a $6000\,\mathrm{g\,mol^{-1}}$ PDMS). This range of ultra-thin membrane thickness is more adapted for a multi-layered stack configuration (figure 2 B), as it does not require to have freestanding suspended membranes.

B. Compliant electrodes

Compliant electrodes are a key element to DETs. They are required to bring and remove the electric charges on the surface of the membrane, but can negatively impact the performance of a device, for example by mechanically stiffening the structure or limiting the electrical charging time. Most larger scale DEA lab prototypes have electrodes made of grease, carbon black powder, or carbon nanotubes, manually applied on the surface of the membrane[39]. These approaches lead to electrodes that can be easily damaged and have a short lifetime. They are therefore not suitable for smaller scale devices, keeping batch fabrication, reliability and reproducibility in mind. In this prospect, it is important to have electrodes that are solid and that present a good adhesion to the membrane in order to prevent mechanical abrasion. Suitable electrodes include conductive rubber made by dispersing conductive particles (such as carbon black) into an elastomer[75,103,104], or soft ionic gels[105,106]. Multilayer actuators can use electrodes made of loose particles, as the electrode will be encapsulated by the next dielectric layer (see e.g.[107]).

When miniaturizing DETs, two different issues must be taken into account. First, small lateral dimensions make the application of the electrodes by hand impossible, especially in the context of mass fabrication. Effective patterning methods are therefore required. Different solutions exist using shadow masks, photolithography or stamping, and are reviewed in more details elsewhere[39]. Second, in case the membrane is scaled down, the electrodes must be applied without damaging the very thin elastomer.

This is particularly problematic for the surface expansion configuration (figure 2 A), as the electrodes are applied on a suspended membrane that can be easily damaged. Patterning techniques involving mechanical contact (such as stamping) are therefore unsuitable when the membrane becomes too thin. Spraying though a shadow mask is also problematic because of the contact between the mask and the membrane (it can be suspended above the surface, at the cost of resolution), as well as the deformation of the film induced by the air flow. Inkjet printing is the optimal solution as it allows patterning the electrode on the thin membrane without touching it or deforming it.

To produce their thin printed actuators (c.f. section III A), Poulin et al. have stamped the electrodes before releasing the membrane from the substrate on which it was applied[100]. Because the membrane is still fixed on a hard backing, it is not damaged by the stamping process. After release from the substrate, a DET structure is obtained by bonding two membranes with a stamped electrode back to back[100].

An additional impact of scaling down the elastomer thickness is the increase of stiffening impact of the electrodes. Indeed, electrodes suitable for small scale devices (particles in an elastomer matrix, ionogels, etc.) behave as an elastic solid and store mechanical energy when deformed. They therefore reduce the actuation strain compared to the ideal case given by equation 1. Scaling down the thickness of a DET usually concerns the membrane only, as the electrodes are already made as thin as possible. The stiffening impact of the electrodes depends on the ratio between the electrode and the membrane thicknesses. Thin DETs can therefore be negatively impacted if the electrodes are not carefully engineered. The impact of the electrodes on strain is discussed in more details in section IV B.

C. Single layer surface expansion actuators

Single layer surface expansion actuators (figure 2 A) are the most widely used DEA configuration. In its most widespread form, the devices consist of a VHB membrane prestretched on a frame, with hand-applied carbon grease electrodes (see e.g.[6,10,18,62]). Although this fabrication method is well adapted to the production of large-scale prototypes ($>1\,\mathrm{cm^2}$), it is not suitable for the reproducible manufacture of a large quantity of devices of smaller size. Miniaturized devices require precisely patterned electrodes that exhibit good adhesion to the membrane and resistance to mechanical abrasion, as well as membranes with controllable mechanical parameters and thickness (c.f. sections III A and III B).

Rosset et al. have recently published an article detailing the complete production process of a single layer surface expansion actuator based on a silicone membrane. The process describes silicone membrane casting on A4-size substrates, prestretching, and patterning of compliant electrodes by pad printing[103]. Although still at a lab scale, this production method presents large improvements compared to manual fabrication, including large area membrane coating that allows making many actuators from a single membrane, or the rapid and precise patterning of the electrodes. Because it uses a stamping technique to precisely pattern the electrodes, the method is well adapted for scaling down the in-plane dimensions. But being a contact method, it requires membranes that are at least $10\,\mu\mathrm{m}$ thick. Thinner membranes would require either a non-contact patterning method, applying the electrodes before the membrane is released from its casting liner[100], or using a transfer technique[92].

D. Layer-by-layer stacked actuators

Applications that make use of the thickness compression of the membranes usually require stacked actuators in order to reach usable absolute displacements. Because of the large number of layers that need to be stacked (from about 20 to >500), stacked actuator fabrication must be fully automated. The group of Prof. Schlaak from TU Darmstadt has developed a process to fabricate stacked DEAs. It consists of a sequence of three operations: spin coating of a thin silicone layer, cross-linking of the elastomer layer, and electrode spraying through a shadow mask (graphite powder dispersed into isopropanol)[107]. This method has been used to fabricate some of the devices mentioned in section II, such as a tactile interface (40 layers of 30 µm)[54], a peristaltic pump (30 layers of 50 µm)[87], or a tuneable lens (30 layers of 45 µm)[58].

In a layer-by-layer process, the different layers are produced on top of the previous one. Silicone layers are therefore applied on top of the previous electrode. Particle-based compliant electrodes are generally not very smooth, and it is important to apply a silicone layer that is thick enough to avoid pinholes in the membrane. Consequently, the minimal thickness of the dielectric is limited by the roughness and thickness of the electrodes. The fabrication process for a single layer must have a high yield, in order to have a functional actuator after stacking many layers on top of each other. In a study about using DEAs for artificial urinary sphincters, Müller et al. note that to keep the driving voltage to acceptable levels (24 V), the dielectric should be submicrometer thick, and that it would then require to have a stack of >1000 layers to obtain the desired force[82]. Even with a production yield per layer as high as 99.8 %, the yield of a 1000-layer actuator would only be 13.5 %. One solution to this problem is to limit the serial production to a smaller number of layers, such as 20 to 50. Each unit can then be electrically tested, discarding those who present premature dielectric breakdown. Finally, an actuator can be assembled by stacking several functional sub-units on top of each other.

The layer-by-layer fabrication process is used by the Swiss company CTsystems[108], which produces stacked DEAs for industrial applications such as pneumatic valves[52]. The serial production process consists in the successive deposition of 25 µm silicone membranes, followed by the patterning of graphene-based electrodes (≈300 nm) over a large area. The process is repeated until a stack of 21 silicone layers is obtained, after what the large produced surface containing many sub-units is cut into 15 mm × 15 mm modules that are electrically tested. 38 modules are then stacked on top of each other to form a 20 mm tall actuator that has 798 layers in total[109].

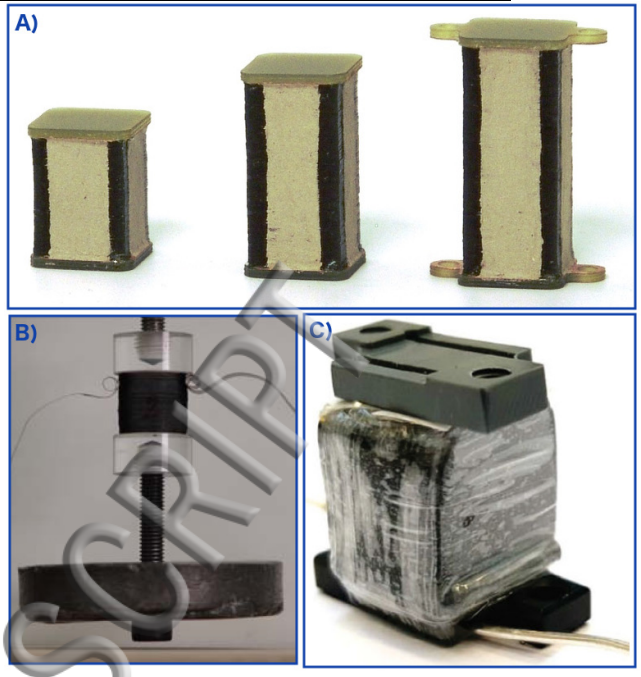

FIG. 11. Examples of contractile stacked actuators manufactured by automated processes. A) 15 mm × 15 mm actuators of different height from the company CTsystems, Switzerland. ©2016 CTsystems. Reproduced with permission. B) diameter 20 mm stacked actuators from EMPA, Dübendorf Switzerland[110]. ©2009 Elsevier Ltd. Reprinted with permission. C) 10 mm × 10 mm stacked actuators made by folding and stacking from HS-OWL, Germany[111]. ©2015 Springer Science+Business Media. Reprinted with permission.

E. Stacked actuators with pre-made membranes

One of the principal limitations of stacked actuators produced layer by layer (c.f. section III D) is that – except for the first layer – the liquid elastomer precursor is applied on the previous layer and electrode, i.e. on an imperfect surface that presents thickness inhomogeneities and non-negligible surface roughness. This has the consequence of either decreasing the fabrication yield, or of limiting how thin the dielectric membrane can be made.

An alternative way of fabricating stacked DETs is to use a pre-made membrane. A large-area membrane is fabricated separately on a casting liner that has no defects and a very low surface roughness. This enables the production of thin high-quality membranes, with a low defect density. The compliant electrodes are then patterned on the membrane. Many electrode can be patterned on a single large-area membrane, allowing parallel fabrication (figure 12 A). The membrane is cut to separate each of the sub-units (figure 12 B). Finally, the sub-units are stacked on top of each other to form a stacked actuator (figure 12 C). In practice, it is often easier to first stack a few full membranes with electrodes (figure 12 A) on top of each other, and then cut them into sub-units that are stacked to form the final device. To increase fab-

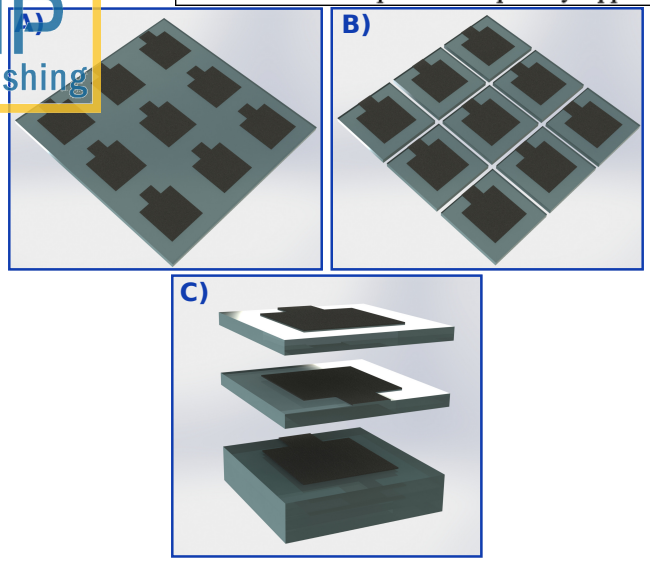

FIG. 12. Parallel fabrication of a stack actuator. A) An array of electrodes is patterned on a membrane. B) The membrane is cut into sub-units. C) the sub-units are stacked on top of each other.

rication yield, modules of a few layers can be fabricated and electrically tested, before stacking several modules on top of each other.

This fabrication process has been used by Kovacs et al. to manufacture stacked actuators capable of contracting by 2.5 mm (10 % of original length) while lifting a mass of 2.11 kg[110]. This represents a mechanical work of 52 mJ or an energy density of 12.9 J kg^{-1}. Two techniques have been used to assemble the devices: a handcrafted fabrication, similar to the process described on figure 12, and an automated stacking process using a purpose-built machine[112]. The membranes used for the actuators is an interpenetrating polymer network based on a VHB acrylic tape[113].

When a voltage is applied, the electrostatic force holds the layers together, provided the electrodes are thin and can sustain the traction force. For this reason, it is important that the electrodes are very thin, ideally a monolayer[110]. In the absence of voltage, there is no force to hold the layers together. If the device must sustain tensile loads, it must be designed or packaged accordingly. McKay et al. have solved this problem by using oxygen plasma bonding to provide adhesion between the different layers for their miniature stacked generator based on silicone membranes[14]. The oxygen plasma bonding between the layers allows them to sustain tensile deformation without breaking apart.

Instead of cutting the membrane into sub-units and stacking them on top of each other, a folding process can be used to manufacture multi-layer actuators. The process was first introduced by Carpi et al. who produced long bands of silicone film coated with compliant electrodes that were then manually folded into a stacked actuator[114].

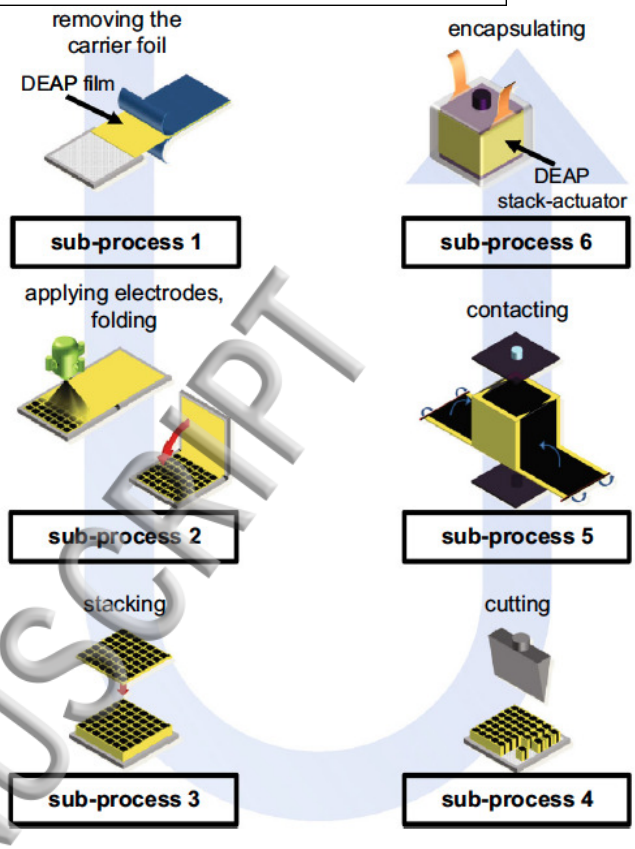

FIG. 13. Automated multi-layer stacked actuator fabrication based on a folding process[111]. ©2015 Springer Science+Business Media. Reprinted with permission.

Maas et al. have developed a completely automated process to produce folded actuators from commercial rolls of elastomer films[111]. The fabrication is separated into 6 sub-processes (figure 13): 1) The elastomer film is separated from its casting liner and protection foil without stretching the film and cut into 200 mm × 400 mm membranes. 2) An array of electrodes is sprayed through a shadow mask on half of the surface, followed by folding the membrane in two. In total, 4 electrode applications and 3 folding steps are performed to obtain an eight-layer 100 mm × 100 mm block. 3) Several of these blocks are stacked on top of each other until the desired total thickness is obtained. 4) A 100 mm × 100 mm block typically contains many smaller sub-units that were fabricated in parallel during the spraying/folding step. These sub-units are separated by cutting the block along two orthogonal directions using an ultrasonic knife. 5) A layer of elastomer film with conductive tracks is applied around each actuator to provide electrical contact to the electrodes. 6) The actuators are encapsulated. The process has been tested with commercial polyurethane (PUR) and silicone films to assemble actuators with 200 layers and an active surface of 64 mm. When a 50 V µm^{-1} field is applied, the PUR actuators exhibit an unloaded strain of 3.5 % and a blocking force of 10 N, and 3 % / 4 N for

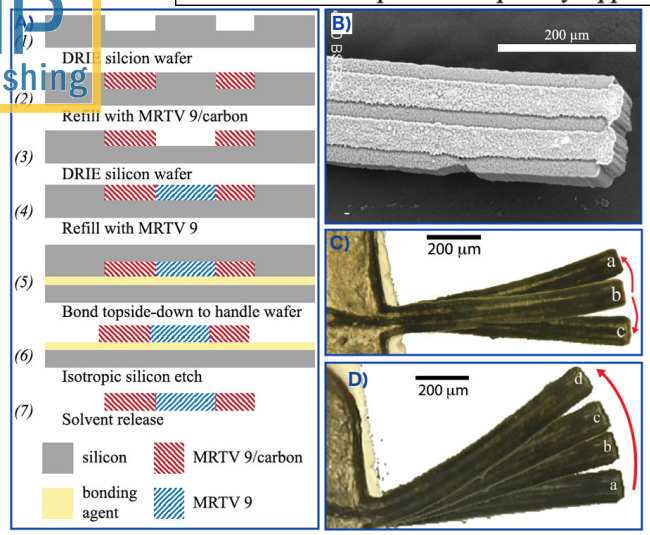

FIG. 14. A) MEMS-inspired DEA fabrication process. B) SEM picture of bilayer bending actuator after release. C) Bidirectional actuation depending on which pair of electrode is activated. D) Unidirectional actuation for voltages from 0 V to 1100 V[117]. ©2014 IOP publishing. Reproduced with permission. All rights reserved.

the silicone actuators[111].

F. MEMS-inspired production process

Fabricating DETs at the sub-mm scale imposes additional constraints to the fabrication process[115]. Some fabrication steps – such as prestretching – become difficult or impossible to integrate in a MEMS-inspired fabrication process, thus limiting the actuator configurations that can be realized at smaller scale[115].

Gerratt et al. have developed a process to integrate PDMS with silicon structures in a traditional microfabrication approach[116]. The process involves dry etching of trenches in a Si wafer, which are then filled with PDMS before releasing the suspended structures. It enables the fabrication of structures that take advantage of the mechanical properties of PDMS, such as soft hinges. This method has been used to fabricate bilayer bending DEAs (figure 14)[117]. Trenches are patterned by deep reactive ion etching (DRIE) into a Si wafer and filled with a conductive silicone elastomer. After curing and removal of the excess of PDMS, a second set of trenches are patterned by DRIE in between the conductive silicone zones. The trenches are filled with pure silicone, and the excess is scraped off after curing. Finally, the Si mould is etched away to release the structures. The bending actuators are 1 mm long, and are formed by 5 layers (3 electrodes and 2 dielectrics) of 20 µm. A deflection of the tip of 318 µm is observed for an applied voltage of 1100 V[117].

Compared to the other stacked actuator fabrication techniques presented earlier (c.f. sections III D and III E), for which the layers are added on top of each other horizontally, the micro-molding procedure of Gerratt et al. creates layers vertically in the Si master. The process – demonstrated here for a bilayer actuator – can easily be extended to many more layers. Because of the vertical fabrication, increasing the number of layers doesn't increase the number of steps: 3 steps (etching, filling, scraping the excess) are required for the electrodes, irrespective of the number of layers, and the same applies for the dielectric layer.

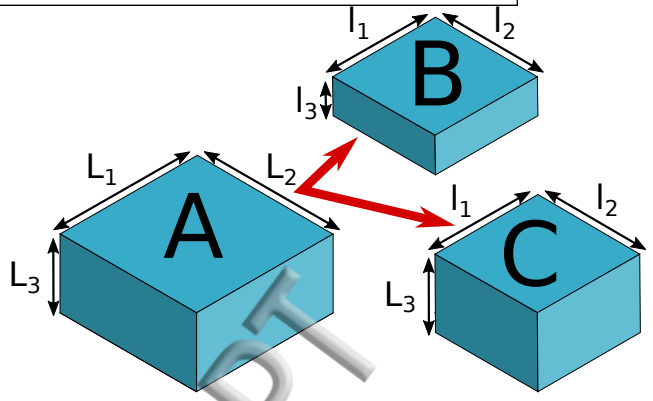

FIG. 15. Scaling down a DEA. From original dimensions L_1, L_2, L_3 (A), the device is miniaturized either to dimensions l_1, l_2, l_3 (isotropic scaling, B), or to dimensions l_1, l_2, $l_3 = L_3$ (in-plane scaling, C).

IV. PERFORMANCE MODELS

A. Effect of scaling down

Scaling down the dimensions of DEAs impacts their performance. If the influence on displacement or force is quite straightforward, other effects – such as the role of the electrodes or boundary conditions – are less obvious and can negatively affect the actuators. Here, we consider a DEA of dimensions L_1, L_2, L_3, which is miniaturized to l_1, l_2, l_3 (figure 15). Because it may not always be possible or desirable to decrease the thickness of the membrane, we consider two different cases:

- Isotropic scaling: scaling in all directions: $l_1/L_1 = \alpha$, $l_2/L_2 = \alpha$, $l_3/L_3 = \alpha$
- In-plane scaling: scaling in-plane only: $l_1/L_1 = \alpha$, $l_2/L_2 = \alpha$, $l_3/L_3 = 1$

The key metrics of the actuators for these two cases with respect to the scaling parameter α are given in table I for a constant electric field ($\alpha < 1$ for miniaturization). In this section, we neglect the impact of the electrodes (i.e. we consider them to be perfectly compliant. The case of realistic electrodes is discussed in details in section IV B). The impact of the thickness reduction in isotropic scaling can be compensated by increasing the number of

TABLE I. Effect of scaling on strain, displacement, blocking force and driving voltage for a constant electric field for the surface expansion and thickness compression configurations.

Actuator	surface exp.		thickness comp.	
scaling	Isotropic	in-plane	isotropic	in-plane
Strain	1	1	1	1
Displacement	α	α	α	1
Force	α^2	α	α^2	α^2
Voltage	α	1	α	1
Capacitance	α	α^2	α	α^2
Energy dens.	1	1	1	1

layers by a factor $1/\alpha$ to obtain the same behavior as in-plane scaling for strain, displacement and blocking force, while keeping the driving voltage at a factor α. Depending on the type of scaling, the capacitance of the device scales down as α, or even α^2. Sensing applications are therefore more delicate at small size-scale, because the device capacitance becomes small in comparison to parasitic capacitances introduced by contacts and cables, thus making the detection of small deformation difficult. The energy density of DETs is independent of their size, thus making them interesting at largely different size scale, from the blimp to the cell-stretching device, as stated in the introduction.

The response speed and resonance frequency are also important parameters for a DEA. The spring constant of the device depends on how the device is used and how the scaling is done (isotropic or in-plane), but generally scales as α or α^0. The mass scales as α^3 (isotropic scaling), or α^2 (in-plane scaling), and is therefore the dominating factor for the resonance frequency of the system ($f = (k/m)^{0.5}$). Consequently, miniaturized devices have higher mechanical resonance frequencies. Small DEAs can therefore display faster response speed, provided their electrodes are conductive enough so that their electrical cut-off frequency is higher than the mechanical resonance frequency.

As an illustration, consider a DEA rotary motor, as introduced by Anderson et al. Their device has a diameter of 200 mm, with a shaft turning at 2 Hz to 3 Hz[118]. A miniaturized version of the motor made on a diameter 20 mm membrane turns at 25 Hz, with the electrodes being activated at several hundreds of Hertz[104]. As a second example, the silicone lens from Maffli et al.[70] exhibits a settling time <200 µs, thanks to the small size and small mass of liquid that needs to be moved (cf. section II B): miniaturized soft system can also be fast.

B. Effects of the boundary conditions

Electrodes can strongly impact the performance of DEAs when the thickness of the membrane is reduced. As mentioned above (c.f. section III B), most reliable

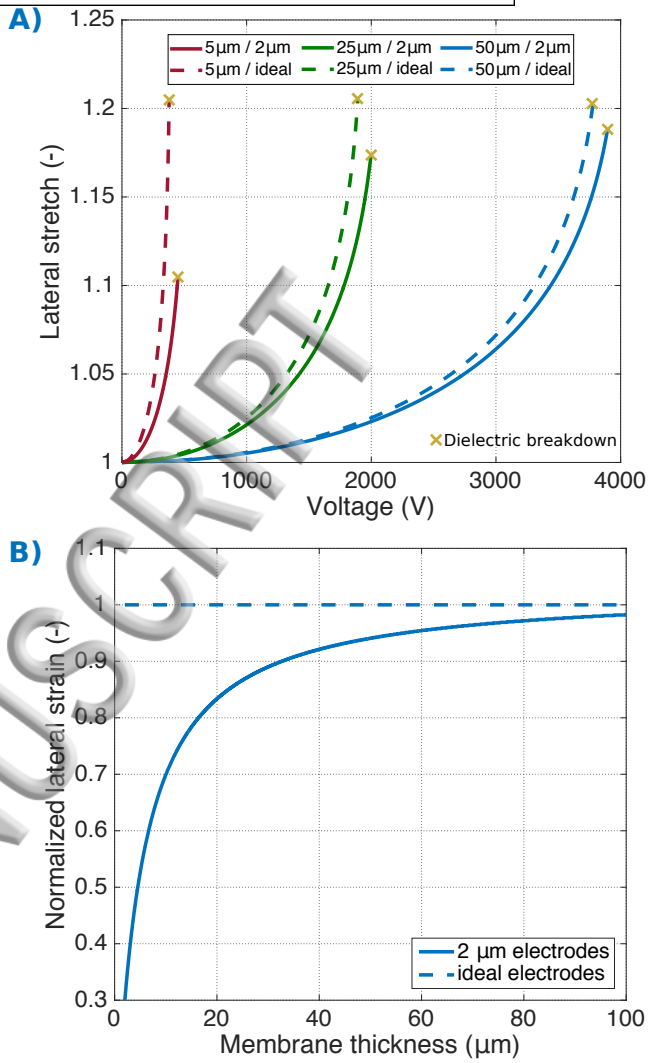

FIG. 16. A) Lateral stretch as a function of the applied voltage for different membrane thicknesses, and considering either ideal electrodes, or 2 µm-thick electrodes with the same mechanical properties as the membrane. Devices with realistic electrodes exhibit less strain at the same voltage compared to ideal electrodes, and a lower maximal stretch at breakdown. B) Normalized lateral strain at a fixed electric field for the same situation as above. The strain of thin membranes is much impacted by the electrodes.

electrodes behave as elastic solid and store energy when deformed. Additionally, the thickness of the electrodes generally does not scale down with the thickness of the membrane, as they are usually made as thin as possible. Consequently, the thinner the dielectric membrane, the larger the relative volume of the electrode becomes, with a negative impact on strain. From equation 1, we expect that scaling the membrane thickness by a factor α leads to a scaling $1/\alpha$ in driving voltage, but this only holds with perfectly compliant electrodes (either infinitely thin, or with a Young modulus of 0).

Poulin et al. have developed a model based on hy-

perelastic energy density functions to predict the strain of DEAs while taking the impact of the electrodes into account[41,119]. As an example, we consider a simple single layer in-plane expanding circle actuator, with free boundary conditions. The mechanical properties of the membrane are modeled using the Gent hyperelastic energy density function[120] with parameters $\mu = 0.3$ MPa and $J_m = 20$. The electrodes are assumed to have the same mechanical properties as the membrane, and a thickness of 2 µm. The lateral stretch versus applied voltage is shown in figure 16 a for three different membrane thicknesses. Compared to ideal electrodes, realistic electrodes cause a decrease in actuation stretch for a fixed applied voltage, as well as a decrease of the maximal stretch at dielectric breakdown (set at 110 V µm^{-1} for this example). Both effects become more and more important for thinner dielectric membranes. Figure 16 B shows the normalized lateral actuation strain at a fixed electric field as a function of membrane thickness. While for ideal electrodes the strain as a function of the electric field does not depend on membrane thickness (equation 1), realistic electrodes can have a dramatic impact at small membrane thickness. This becomes particularly problematic when the membrane thickness becomes comparable to the electrode thickness, which is likely to happen when miniaturizing DEAs (see e.g. figure 14 B).

These considerations demonstrate that scaling down the dielectric thickness of DETs puts much more constraints on the mechanical properties of the electrodes. They must be as soft and thin as possible, while still being conductive enough to not limit the response speed. Although fabrication methods for sub-micrometer membranes have been demonstrated[101,102], solutions for compliant electrodes adapted to these membranes do not exist yet. In addition to extreme compliance, they should also exhibit good adhesion to the membrane, absence of degradation with time and when cyclically stretched, and there should be an appropriate technique to pattern them on the membrane without damage.

Another important limiting factor of miniaturized DEAs is the impact of the passive zone of the membrane (i.e. the zone which is not coated with electrodes), particularly for the case of area expansion actuators based on prestretched membranes. Analytical modeling of DEAs, show that having a constant external force pulling on a DEA enhances its performance[49,121]. Large-scale actuators can make use of dead weights to provide this constant force[49,121]. However, weights attached to the membrane with strings are highly impractical for small-scale devices, which must be able to work in any orientation, not to mention the difficulty to attach wires to the membranes in an automated way. Consequently, small-size DEAs usually rely on passive areas of the membrane to provide the counter-balancing force. This configuration is used for example when a rigid object located on the surface of the membrane must be translated by the action of the electrodes, such as in Optotune's Laser speckle reducer[67] (c.f. section II B), Artificial Muscles' haptic feedback device[4] (c.f. section II A), or mm-wave radio-frequency phase shifters developed at EPFL[122]. However, unlike the situation with a dead weight providing a constant force, the mechanical tension in the passive zone relaxes as the active area expands, causing a decrease in internal force and a reduction of actuation strain compared to the constant force case. Rosset et al. have analyzed the impact of the passive zone for miniaturized actuators, with the aim of maximizing the displacement of a rigid object placed on the DEA for a fixed actuator size[123]. The authors show that the optimal situation to maximize the absolute displacement is to have an electrode and passive membrane of equal size, and that the obtained displacement is half as much as in the constant force case due to the stress relaxation in the passive zone.

Larger scale actuator also often use the passive membrane as a way to produce a counter-force to the active area. But the passive zone is made large compared to the active region so that when the electrodes expands, the force in the passive area remains approximately constant. Koh et al. have demonstrated that for expanding dot actuator, a ratio larger than 10 between the total size of the membrane and the size of the central active part ensures that the passive zone of the membrane doesn't restrict actuation or cause loss of mechanical tension[89]. However, this approach is hardly compatible with miniaturization, whose goal is to reduce the overall size of the devices: either the actuator is small, or it is made of a large membrane on which many independent actuators are patterned. In either case, the spacing between an active zone and the holding frame (or the neighboring actuators) is likely much smaller than 10 times the size of the electrode, thus reducing the strain compared to the ideal cases often studied in the literature.

V. INCREASING THE FORCE

Dielectric elastomer transducers present many key parameters that make them interesting for miniaturization: low-power consumption, large strains, fast response speed, high energy density and simple architecture. But they suffer from two important drawbacks. 1) The high voltage required to drive them. This makes the control electronics expensive and bulky, which goes against the idea of miniaturization and large-scale production. However, miniaturization of the membrane thickness can alleviate this problem. 2) The low force produced by surface-expansion transducers, particularly when the membrane thickness is also scaled down (c.f. table I). Different approaches can be taken to mitigate this issue, such as using external passive elements, or using hybrid actuators to benefit from the large strain of DETs, together with strong blocking force provided by other means. One such hybrid actuator, a versatile gripper combining a DEA for the open/close motion and electro-adhesion for the holding force has been mentioned before (c.f. section II C). A few other approaches are discussed below.

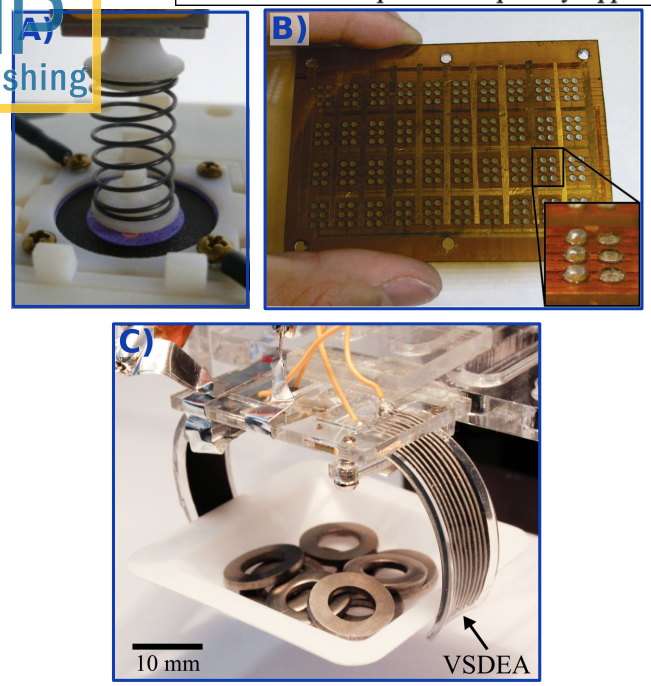

FIG. 17. Different approaches based on hybrid configurations to increase the output force of a DEA. A) Diaphragm actuator biased with a spring[124]. ©2013 IOP publishing. Reproduced with permission. All rights reserved. B) Braille cell array based on phase-changing DEAs, leading to bistable operation and high holding force. From[125]. ©2012 SPIE. Reproduced with permission. C) Gripper made with a bending DEA with a low-melting-point-alloy meander in the elastomeric substrate. Joule heating allows controlling the stiffness of the substrate by liquefying or solidifying the metal[30]. ©2015 IEEE. Reproduced with permission.

A. Stacked surface expansion actuators with a biasing mechanism

Surface expansion actuators usually have large displacements and low force, while thickness compression actuators are known for their high forces and small displacement. The Seelecke group from Saarland university has produced actuators based on surface expansion that combine large stroke and high output force by stacking a few membrane layers and using biasing springs (figure 17 A)[126]. Unlike thickness compression stacked actuators, which usually comprise several hundred layers, they have stacked 18 membranes with annular-shaped electrodes. The central part of the membranes is pushed out of plane by a combination of a linear spring and a negative-rate bias (NBS) spring (figure 18. The two springs and the active membrane are carefully designed to achieved the desired bistable behavior combining large stroke and large force[124]. The actuator and biasing mechanism hold in a 85 mm × 85 mm × 35 mm enclosure, and the device can lift a weight of 7.5 kg by 2.25 mm[126]. A particular attention has also been paid to the fabrication process, which is based on automated industrial techniques, such

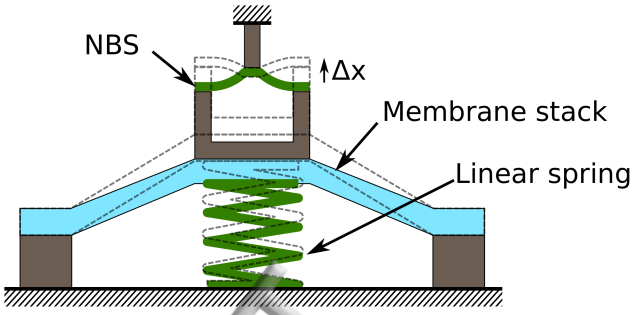

FIG. 18. Principle of a diaphragm actuator with biasing mechanism. Both springs (linear spring and negative-rate bias spring) work with the active stack of membranes to provide bistable actuation with a large output force. The actuator is shown at rest, while the dashed outline shows the configuration when a voltage is applied and the NBS has snapped in its second stable configuration.

as screen printing to apply carbon-filled electrodes and frames, or rapid 3D manufacturing techniques[127].

B. Variable stiffness actuators

Their large strain, compactness and possibility to manufacture arrays make DEAs attractive for Braille displays. However, in addition to a large displacement (>500 µm[128]) a Braille dot must also be exhibit a large holding force (>150 mN[128]), outside of the capabilities of surface-expansion actuators. The Pei group from UCLA has solved the problem by using a shape memory polymer (SMP) as the dielectric membrane of a DEA (figure 17 B)[28,47]. The most recent material they developed exhibits a change of storage modulus of a factor of 1000 when heated by about 10 °C[28]. The material behaves as an elastomer in the heated state, and as a hard plastic when cooled down. The SMP has been used to make DEA diaphragms that bulge out of plane when activated. A small air pressure is applied below the diaphragm, which is placed in an oven at 50 °C. An electric field up to 127 V µm^{-1} is applied to the diaphragm, leading to out of plane deflection corresponding to an area strain up to 70 %[28]. After the actuator is removed from the oven and has cooled down, the voltage can be removed and the actuator keeps its deformed state. Because the membrane is in a hard state it can sustain the force of a finger. The principle of these bistable diaphragm actuators has been applied to make a page-size 18 × 18 cells Braille device, although not individually addressable[47].

A SMP dielectric membrane enables the combination of the large actuation stroke provided by surface-expansion DEAs, with large holding forces resulting from the high Young modulus of the material in its cold state. This opens the door to a broad new range of applications requiring stroke and holding force at the same time, such as Braille displays. However, another impor-

tant requirement for this application is the ability to address each pin individually (the 18×18 cells prototype from[129] has 1944 actuators). High voltage switches (transistors) are voluminous and expensive, and are therefore a major drawback for applications requiring large arrays of independent DEAs. Besse et al. have recently introduced a concept for a SMP-based tactile display in which electrodes patterned on a SMP membrane are used as independently-addressable micro-heaters[Besse2016]. The voltage required for the Joule heating being in the order of 20 V, standard electronic components can be used. Furthermore, a row-column addressing scheme is used to decrease the number of switching elements. In this particular example, the up and down motion of the diaphragms is provided by a miniaturized pump and not a DEA. However, the same approach can be used with a DEA replacing the pump, the key point being that a single high voltage channel is necessary: the addressing is performed by selecting which units are heated, while the high voltage is applied to all devices in parallel, thus requiring a single channel.

As an alternative to SMP, Shintake et al. investigated the use of a low-melting-point alloy (LMPA) to change the stiffness of a bending DEA[30]. The device consists of a thick (1 mm) silicone substrate with an embedded micro-channel filled with LMPA. A prestretched DEA is then bonded on top of the substrate. When a current is applied to the LMPA meander, the joule heating causes it to melt, thus leading to a decrease in stiffness of the entire structure by a factor of 11. In the heated state, a voltage applied to the DEA allows to tune the bending angle. The desired position can then be locked by stopping the current flow in the LMPA resistance. The DEA control voltage can then be removed while the actuator keeps its actuated shape. Two of these LMPA/DEA structures were combined to form a 2-finger gripper which is able to lift a weight of 11 g for a total weight of active material of 2 g (figure 17 C)[30129].

VI. CONCLUSIONS

One of the remarkable properties of dielectric elastomer transducers is that their energy density is invariant over a size scale of several orders of magnitude (table I). This is in contrast with other types of actuation mechanisms whose performance can be negatively impacted by scaling. For example, electromagnetic actuators suffer from down-scaling because of Joule losses and core saturation, and it is difficult to scale up air-gap electrostatic actuators because of the reduced breakdown field at higher gap values. This scale-invariance in energy density renders dielectric elastomers attractive for inclusion in applications of vastly different sizes, from square meters of actuators in the case of a biomimetic blimp, to actuators sub-millimeter devices for biomedical applications (figure 1).

Applications of the technology for miniaturized devices has a bright future, due to the chief advantages of DETs: large strains, large energy densities, compliance, etc. However, some key challenges remain to be solved before DETs find their way in every consumer product. Indeed, although simple models predict that the actuation strain of DEAs is size-independent (equation 1, table I), miniaturized devices generally exhibit a lower actuation strain due to a number of factors. The stiffening impact of electrodes reduces the strain, and the unavoidable defects in thinner dielectric membranes limit the electric field that can be applied before breakdown which further limits the maximal performance of thin devices. The high driving voltage is another important obstacle to the widespread use of DETs. Miniaturization of the membrane thickness is one possible route towards lower actuation voltage that would render the technology compatible with standard electronics components and ease their integration. The fabrication of miniaturized DETs consequently requires new production processes capable of high-yield, high-quality reliable, reproducible and automated batch fabrication.

ACKNOWLEDGMENTS

The authors would like to thank the many authors who have accepted to share their results with us and agreed to the use of their pictures and figures. Many thanks to Alexandre Poulin for his valuable input.

[1] R. F. Shepherd, F. Ilievski, W. Choi, S. A. Morin, A. A. Stokes, A. D. Mazzeo, X. Chen, M. Wang, and G. M. Whitesides, Proceedings of the National Academy of Sciences of the United States of America **108**, 20400–20403 (2011).

[2] J. Shintake, S. Rosset, B. Schubert, D. Floreano, and H. Shea, Advanced Materials **28**, 231 (2016).

[3] A. D. Marchese and D. Rus, The International Journal of Robotics Research (2015), 10.1177/0278364915587925.

[4] S. J. Biggs and R. N. Hitchcock, in *Proceedings of SPIE - The International Society for Optical Engineering*, Vol. 7642 (2010) pp. 76420I–76420I–12.

[5] M. Matysek, P. Lotz, T. Winterstein, and H. Schlaak, in *Proceedings - 3rd Joint EuroHaptics Conference and Symposium on Haptic Interfaces for Virtual Environment and Teleoperator Systems, World Haptics 2009* (2009) pp. 290–295.

[6] G. Frediani, D. Mazzei, D. E. D. Rossi, and F. Carpi, Front. Bioeng. Biotechnol. **2** (2014), 10.3389/fbioe.2014.00031.

[7] H. A. Sonar and J. Paik, Frontiers in Robotics and AI **2** (2016), 10.3389/frobt.2015.00038.

[8] F. Carpi, G. Frediani, S. Turco, and D. De Rossi, Advanced Functional Materials **21**, 4152 (2011).

[9] S. Shian, R. M. Diebold, and D. R. Clarke, Optics Express **21**, 8669 (2013).

[10] M. Kollosche, S. Doering, J. Stumpe, and G. Kofod, Optics Letters **36**, 1389 (2011).

[11] D.-X. Lu, Y.-L. Zhang, D.-D. Han, H. Wang, H. Xia, Q.-D. Chen, H. Ding, and H.-B. Sun, Journal of Materials Chemistry C **3**, 1751 (2015).

[12] P. Jean, A. Wattez, G. Ardoise, C. Melis, R. V. Kessel, A. Fourmon, E. Barrabino, J. Heemskerk, and J. P. Queau, in *Proceedings of SPIE - The International Society for Optical Engineering*, Vol. 8340 (2012) p. 83400C.

[13] R. Vertechy, G. P. P. Rosati, and M. Fontana, Journal of Vibration and Acoustics **137**, 011004 (2015).

[14]T. G. McKay, S. Rosset, I. A. Anderson, and H. Shea, Smart Materials and Structures **24**, 015014 (2015).
[15]B. Mosadegh, A. D. Mazzeo, R. F. Shepherd, S. A. Morin, U. Gupta, I. Z. Sani, D. Lai, S. Takayama, and G. M. Whitesides, Lab Chip **14**, 189 (2014).
[16]E. C. Jensen, A. M. Stockton, T. N. Chiesl, J. Kim, A. Bera, and R. A. Mathies, Lab Chip **13**, 288 (2013).
[17]L. Maffli, S. Rosset, and H. R. Shea, Smart Materials and Structures **22**, 104013 (2013).
[18]C. Keplinger, T. Li, R. Baumgartner, Z. Suo, and S. Bauer, Soft Matter **8**, 285 (2012).
[19]P. Maeder-York, T. Clites, E. Boggs, R. Neff, P. Polygerinos, D. Holland, L. Stirling, K. Galloway, C. Wee, and C. Walsh, Journal of Medical Devices **8**, 020934 (2014).
[20]H. A. Baldwin, in *Biomechanics* (Springer Science + Business Media, 1969) pp. 139–147.
[21]E. T. Roche, R. Wohlfarth, J. T. B. Overvelde, N. V. Vasilyev, F. A. Pigula, D. J. Mooney, K. Bertoldi, and C. J. Walsh, Advanced Materials **26**, 1200 (2013).
[22]M. Shahinpoor, Electrochimica Acta **48**, 2343 (2003).
[23]T. Mirfakhrai, J. D. Madden, and R. H. Baughman, Materials Today **10**, 30 (2007).
[24]R. Pelrine, R. Kornbluh, Q. Pei, and J. Joseph, Science **287**, 836 (2000).
[25]P. Brochu and Q. Pei, Macromolecular Rapid Communications **31**, 10 (2010).
[26]I. A. Anderson, T. A. Gisby, T. G. McKay, B. M. O'Brien, and E. P. Calius, Journal of Applied Physics **112**, 041101 (2012).
[27]F. Carpi, S. Bauer, and D. De Rossi, Science **330**, 1759 (2010).
[28]Z. Ren, W. Hu, C. Liu, S. Li, X. Niu, and Q. Pei, Macromolecules **49**, 134 (2016).
[29]R. Altmueller, R. Schwoediauer, R. Kaltseis, S. Bauer, and I. M. Graz, Applied Physics A **105**, 1 (2011).
[30]J. Shintake, B. Schubert, S. Rosset, H. Shea, and D. Floreano, in *2015 IEEE/RSJ International Conference on Intelligent Robots and Systems (IROS)* (2015) pp. 1097 – 1102.
[31]C. Jordi, S. Michel, C. Duerager, A. Bormann, C. Gebhardt, and G. Kovacs, in *Proceedings of SPIE - The International Society for Optical Engineering*, Vol. 7642 (2010) p. 764223.
[32]A. Poulin, C. Saygili, S. Rosset, T. Petrova, and H. Shea, Manuscript submitted to Lab on a Chip (2016).
[33]N. Savage, "Squishy power generators," IEEE Spectrum (2012).
[34]H. Böse, E. Fuss, and P. Lux, in *Proceedings of SPIE - The International Society for Optical Engineering*, Vol. 9430 (2015) p. 943029.
[35]O. A. Araromi, S. Rosset, and H. R. Shea, ACS Applied Materials and Interfaces **7**, 18046 (2015).
[36]F. B. Madsen, A. E. Daugaard, S. Hvilsted, and A. L. Skov, Macromol. Rapid Commun. **37**, 378 (2016).
[37]L. Romasanta, M. Lopez-Manchado, and R. Verdejo, Progress in Polymer Science **51**, 188 (2015).
[38]D. McCoul, W. Hu, M. Gao, V. Mehta, and Q. Pei, Advanced Electronic Materials **2**, 1500407 (2016).
[39]S. Rosset and H. Shea, Applied Physics A: Materials Science & Processing **110**, 281 (2013).
[40]Z. Suo, Acta Mechanica Solida Sinica **23**, 549 (2010).
[41]X. Zhao and Q. Wang, Applied Physics Reviews **1**, 021304 (2014).
[42]T. A. Gisby, B. M. O'Brien, and I. A. Anderson, Applied Physics Letters **102**, 193703 (2013).
[43]T. A. Gisby, B. M. O'Brien, S. Q. Xie, E. P. Calius, and I. A. Anderson, in *Proceedings of SPIE - The International Society for Optical Engineering*, Vol. 7976 (2011) pp. 797620–797620–9.
[44]I. A. Anderson, P. Illenberger, and B. M. O'Brien, in *Proceedings of SPIE - The International Society for Optical Engineering*, Vol. 9798 (2016) p. 97980U.
[45]S. Akbari and H. R. Shea, Sensors and Actuators A: Physical **186**, 236 (2012).
[46]M. Aschwanden and A. Stemmer, in *Proceedings of SPIE - The International Society for Optical Engineering*, Vol. 6524 (2007) pp. 65241N–10.
[47]Z. Ren, X. Niu, D. Chen, W. Hu, and Q. Pei, in *Proceedings of SPIE - The International Society for Optical Engineering*, Vol. 9056, edited by Y. Bar-Cohen (2014) p. 905621.
[48]S. Koh, T. Li, J. Zhou, X. Zhao, W. Hong, J. Zhu, and Z. Suo, Journal of Polymer Science, Part B: Polymer Physics **49**, 504 (2011).
[49]J. Huang, T. Li, C. Chiang Foo, J. Zhu, D. R. Clarke, and Z. Suo, Applied Physics Letters **100**, 041911 (2012).
[50]J. Shintake, S. Rosset, B. E. Schubert, D. Floreano, and H. R. Shea, IEEE/ASME Transactions on Mechatronics **20**, 1997 (2015).
[51]R. Karsten, K. Flittner, H. Haus, and H. F. Schlaak, in *Electroactive Polymer Actuators and Devices (EAPAD) 2013*, Vol. 8687, edited by Y. Bar-Cohen (2013) p. 86870Y.
[52]M. Giousouf and G. Kovacs, Smart Materials and Structures **22**, 104010 (2013).
[53]`www.parker.com`.
[54]M. Matysek, P. Lotz, K. Flittner, and H. F. Schlaak, in *Proceedings of SPIE - The International Society for Optical Engineering*, Vol. 7642, edited by Y. Bar-Cohen (2010) p. 76420D.
[55]M. Matysek, H. Haus, H. Moessinger, D. Brokken, P. Lotz, and H. F. Schlaak, in *Proceedings of SPIE - The International Society for Optical Engineering*, Vol. 7976, edited by Y. Bar-Cohen and F. Carpi (2011) p. 797612.
[56]K. Wei, N. W. Domicone, and Y. Zhao, Optics Letters **39**, 1318 (2014).
[57]C. Keplinger, M. Kaltenbrunner, N. Arnold, and S. Bauer, Proceedings of the National Academy of Sciences of the United States of America **107**, 4505 (2010).
[58]P. Rasti, H. Hous, H. F. Schlaak, R. Kiefer, and G. Anbarjafari, Applied Optics **54**, 9976 (2015).
[59]B. Jin, J.-H. Lee, Z. Zhou, G. Zhang, G.-B. Lee, H. Ren, and C. Nah, Optical Engineering **55**, 017107 (2016).
[60]M. Aschwanden, D. Niederer, and A. Stemmer, in *Proceedings of SPIE - The International Society for Optical Engineering*, Vol. 6927 (2008) pp. 6927–56.
[61]M. Kollosche, S. Döring, G. Kofod, and J. Stumpe, in *Proceedings of SPIE - The International Society for Optical Engineering*, Vol. 7642, edited by Y. Bar-Cohen (2010) p. 76422Y.
[62]S. Rosset, B. M. O'Brien, T. Gisby, D. Xu, H. R. Shea, and I. A. Anderson, Smart Materials and Structures **22**, 104018 (2013).
[63]Z. H. Fang, C. Punckt, E. Y. Leung, H. C. Schniepp, and I. A. Aksay, Appl. Opt. **49**, 6689 (2010).
[64]M. Krishnan, S. Rosset, S. Bhattacharya, and H. Shea, Accepted in Optical Engineering (2016).
[65]M. Aschwanden and A. Stemmer, Optics Letters **31**, 2610 (2006).
[66]`www.optotune.com`.
[67]C. Graetzel, M. Suter, and M. Aschwanden, in *Proceedings of SPIE - The International Society for Optical Engineering*, Vol. 9430 (2015) p. 943004.
[68]M. Beck, R. Fiolka, and A. Stemmer, Optics Letters **34**, 803 (2009).
[69]Q. Zhao, A. Haines, D. Snoswell, C. Keplinger, R. Kaltseis, S. Bauer, I. Graz, R. Denk, P. Spahn, G. Hellmann, and J. J. Baumberg, Applied Physics Letters **100**, 101902 (2012).
[70]L. Maffli, S. Rosset, M. Ghilardi, F. Carpi, and H. Shea, Advanced Functional Materials **25**, 1656 (2015).
[71]M. Wissler and E. Mazza, Sensors and Actuators, A: Physical **134**, 494 (2007).
[72]S. Michel, X. Zhang, C. Wissler, M.and Loewe, and G. Kovacs, Polymer International **59**, 391 (2010).
[73]G. Kofod, W. Wirges, M. Paajanen, and S. Bauer, Applied Physics Letters **90**, 081916 (2007).
[74]M. T. Petralia and R. J. Wood, in *2010 IEEE/RSJ International Conference on Intelligent Robots and Systems* (2010) pp. 2357–2363.
[75]O. A. Araromi, I. Gavrilovich, J. Shintake, S. Rosset, M. Richard, V. Gass, and H. R. Shea, IEEE/ASME Trans-

actions on Mechatronics **20**, 438 (2015).
[76]S. Shian, K. Bertoldi, and D. R. Clarke, Advanced Materials **27**, 6814 (2015).
[77]M. Duduta, R. J. Wood, and D. R. Clarke, Adv. Mater. (2016), 10.1002/adma.201601842.
[78]http://www.flexcellint.com/FX5000T.htm.
[79]S. Akbari, S. Rosset, and H. R. Shea, in *Proceedings of SPIE - The International Society for Optical Engineering*, Vol. 8340 (2012) p. 83401R.
[80]A. Poulin, S. Rosset, and H. Shea, in *Proceedings of SPIE - The International Society for Optical Engineering*, Vol. 9056 (2014) p. 90561Q.
[81]A. Poulin, L. Maffli, S. Rosset, and H. Shea, in *Proceedings of SPIE - The International Society for Optical Engineering*, Vol. 9430 (2015) p. 943011.
[82]B. Müller, H. Deyhle, S. Mushkolaj, and M. Wieland, Swiss Medical Weekly **139**, 591 (2009).
[83]C. W. Senders, T. T. Tollefson, S. Curtiss, A. Wong-Foy, and H. Prahlad, Archives of Facial Plastic Surgery **12**, 30 (2010).
[84]L. G. Ledgerwood, S. Tinling, C. Senders, A. Wong-Foy, H. Prahlad, and T. T. Tollefson, Arch Facial Plast Surg **14**, 413 (2012).
[85]L. M. Fidalgo and S. J. Maerkl, Lab on a Chip **11**, 1612 (2011).
[86]J. J. Loverich, I. Kanno, and H. Kotera, Lab on a Chip - Miniaturisation for Chemistry and Biology **6**, 1147 (2006).
[87]P. Lotz, M. Matysek, and H. Schlaak, in *Proceedings of SPIE - The International Society for Optical Engineering*, Vol. 7287 (2009) p. 72872D.
[88]D. McCoul and Q. Pei, Smart Mater. Struct. **24**, 105016 (2015).
[89]S. Koh, C. Keplinger, T. Li, S. Bauer, and Z. Suo, Mechatronics, IEEE/ASME Transactions on **16**, 33 (2011).
[90]R. D. Kornbluh, R. Pelrine, H. Prahlad, A. Wong-Foy, B. McCoy, S. Kim, J. Eckerle, and T. Low, in *Proceedings of SPIE - The International Society for Optical Engineering*, Vol. 7976 (2011) p. 797605.
[91]https://www.youtube.com/watch?v=G1lMAv-_lqg.
[92]O. A. Araromi, A. Poulin, S. Rosset, M. Imboden, M. Favre, M. Giazzon, C. Martin-Olmos, F. Sorba, M. Liley, and H. R. Shea, Extreme Mechanics Letters (2016), 10.1016/j.eml.2016.03.017.
[93]D. Xu, A. Tairych, and I. A. Anderson, Smart Materials and Structures **25**, 015012 (2015).
[94]J.-Y. Sun, C. Keplinger, G. M. Whitesides, and Z. Suo, Advanced Materials **26**, 7608 (2014).
[95]O. Araromi, A. Poulin, S. Rosset, M. Favre, M. Giazzon, C. Martin-Olmos, M. Liley, and H. Shea, in *Proceedings of SPIE - The International Society for Optical Engineering*, Vol. 9430 (2015) p. 94300Z.
[96]www.youtube.com/watch?v=w-_U0MMoq60.
[97]D. Xu, A. Tairych, and I. A. Anderson, Journal of Polymer Science Part B: Polymer Physics **54**, 465 (2015).
[98]S. Akbari, S. Rosset, and H. R. Shea, Applied Physics Letters **102**, 071906 (2013).
[99]R. E. Pelrine, R. D. Kornbluh, and J. P. Joseph, Sensors and Actuators, A: Physical **64**, 77 (1998).
[100]A. Poulin, S. Rosset, and H. R. Shea, Applied Physics Letters **107**, 244104 (2015).
[101]T. Töpper, F. Weiss, B. Osmani, C. Bippes, V. Leung, and B. Müller, Sensors and Actuators A: Physical **233**, 32 (2015).
[102]F. M. Weiss, T. Töpper, B. Osmani, S. Peters, G. Kovacs, and B. Müller, Advanced Electronic Materials **2**, 1500476 (2016).
[103]S. Rosset, O. A. Araromi, S. Schlatter, and H. R. Shea, Journal of Visualized Experiments , e53423 (2016).
[104]S. Rosset and H. R. Shea, in *Proceedings of SPIE - The International Society for Optical Engineering*, Vol. 9430 (2015) p. 943009.
[105]C. Keplinger, J.-Y. Sun, C. Foo, P. Rothemund, G. Whitesides, and Z. Suo, Science **341**, 984 (2013).
[106]B. Chen, J. J. Lu, C. H. Yang, J. H. Yang, J. Zhou, Y. M. Chen, and Z. Suo, ACS Applied Materials & Interfaces **6**, 7840 (2014).
[107]P. Lotz and H. Matysek, M.and Schlaak, IEEE/ASME Transactions on Mechatronics **16**, 58 (2011).
[108]http://www.ct-systems.ch/.
[109]Personal communication.
[110]G. Kovacs, L. Düring, S. Michel, and G. Terrasi, Sensors and Actuators A: Physical **155**, 299 (2009).
[111]J. Maas, D. Tepel, and T. Hoffstadt, Meccanica **50**, 2839 (2015).
[112]G. Kovacs and L. Düring, in *Proceedings of SPIE - The International Society for Optical Engineering*, Vol. 7287 (2009) p. 72870A.
[113]S. M. Ha, W. Yuan, Q. Pei, R. Pelrine, and S. Stanford, Smart Materials and Structures **16**, S280 (2007).
[114]F. Carpi, C. Salaris, and D. D. Rossi, Smart Materials and Structures **16**, S300 (2007).
[115]B. Balakrisnan and E. Smela, in *Proceedings of SPIE - The International Society for Optical Engineering*, Vol. 7642, edited by Y. Bar-Cohen (SPIE-Intl Soc Optical Eng, 2010) p. 76420K.
[116]A. Gerratt, I. Penskiy, and S. Bergbreiter, Journal of Micromechanics and Microengineering **20**, 104011 (2010).
[117]A. P. Gerratt, B. Balakrisnan, I. Penskiy, and S. Bergbreiter, Smart Materials and Structures **23**, 055004 (2014).
[118]I. Anderson, T. Hale, T. Gisby, T. Inamura, T. McKay, B. O'Brien, S. Walbran, and E. Calius, Applied Physics A: Materials Science and Processing **98**, 75 (2010).
[119]A. Poulin, S. Rosset, and H. R. Shea, in *Proceedings of SPIE - The International Society for Optical Engineering*, Vol. 9798 (2016) p. 97980L.
[120]A. N. Gent, Rubber Chemistry and Technology **69**, 59 (1996).
[121]T. Lu, J. Huang, C. Jordi, G. Kovacs, R. Huang, D. Clarke, and Z. Suo, Soft Matter **8**, 6167 (2012).
[122]O. Araromi, P. Romano, S. Rosset, J. Perruisseau-Carrier, and H. Shea, in *Proceedings of SPIE - The International Society for Optical Engineering*, Vol. 9056 (2014) p. 90562M.
[123]S. Rosset, O. A. Araromi, and H. R. Shea, Extreme Mechanics Letters **3**, 72 (2015).
[124]M. Hodgins, A. York, and S. Seelecke, Smart Materials and Structures **22**, 094016 (2013).
[125]X. Niu, P. Brochu, H. Stoyanov, S. R. Yun, and Q. Pei, in *Proceedings of SPIE - The International Society for Optical Engineering*, Vol. 8340, edited by Y. Bar-Cohen (SPIE, 2012) p. 83400R.
[126]S. Hau, A. York, and S. Seelecke, in *Proceedings of SPIE - The International Society for Optical Engineering*, Vol. 9798 (2016) p. 97980I.
[127]S. Hau, A. York, and S. Seelecke, in *Volume 2: Mechanics and Behavior of Active Materials; Integrated System Design and Implementation; Bioinspired Smart Materials and Systems; Energy Harvesting* (2014) p. V002T02A004.
[128]N. H. Runyan and F. Carpi, Expert Review of Medical Devices **8**, 529 (2011).
[129]https://www.youtube.com/watch?v=y1KcaiKpzXU.

Miniaturization

Actuators

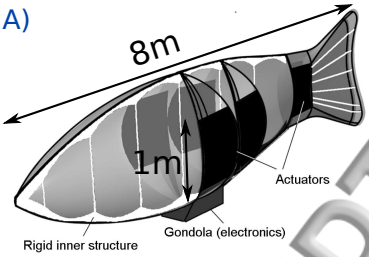

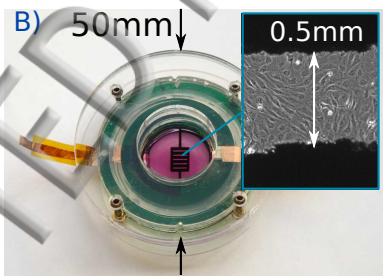

Generators

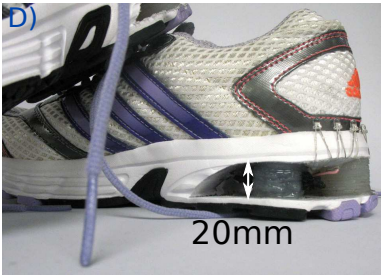

Sensors

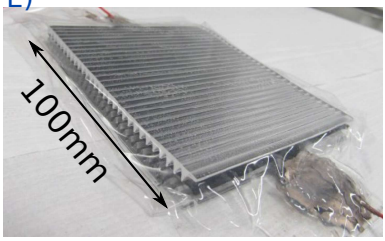

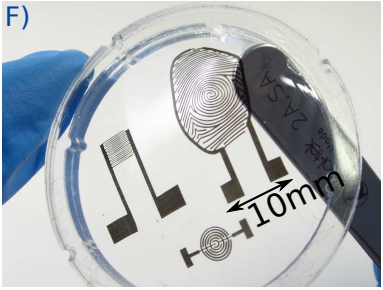

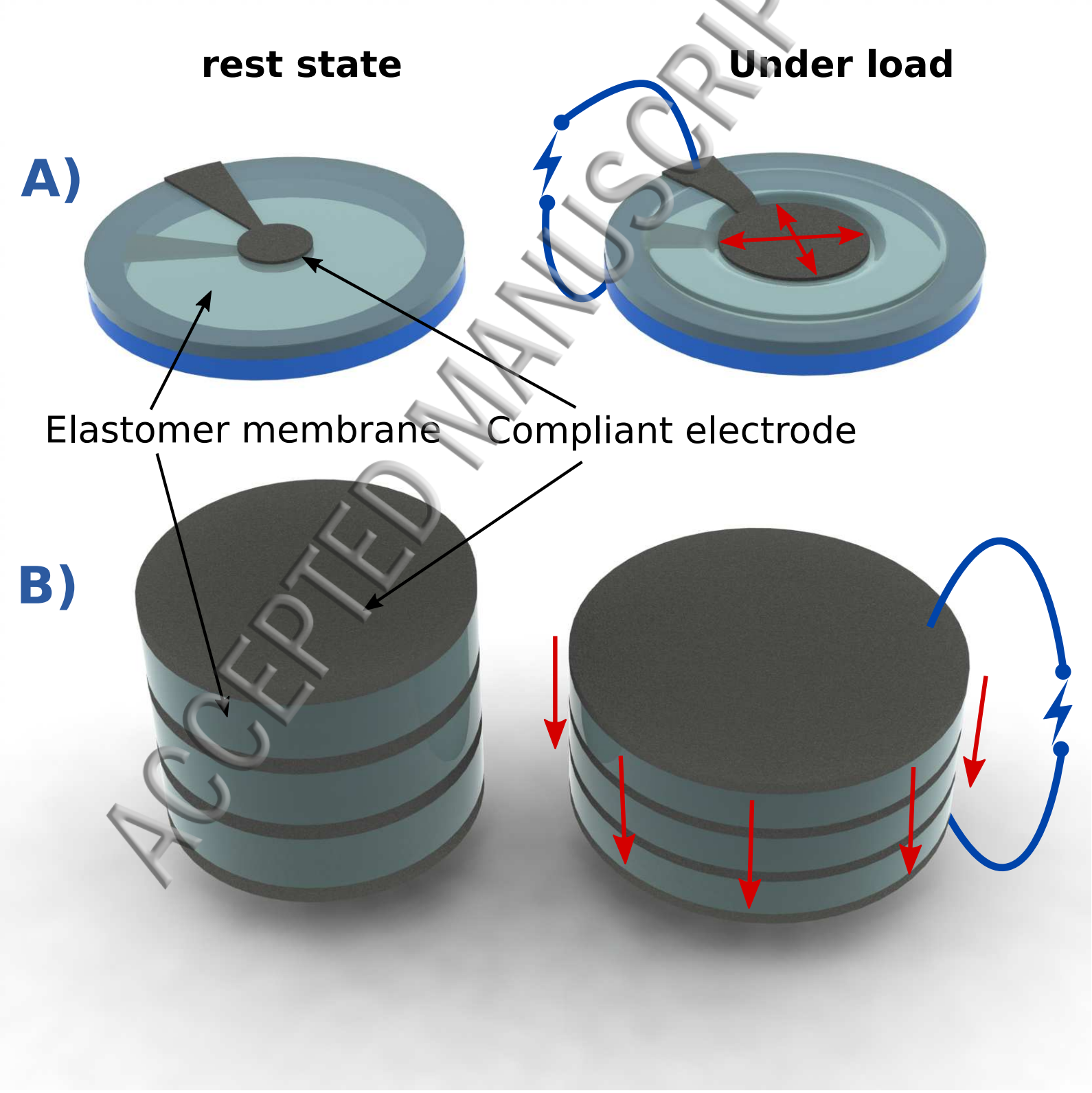

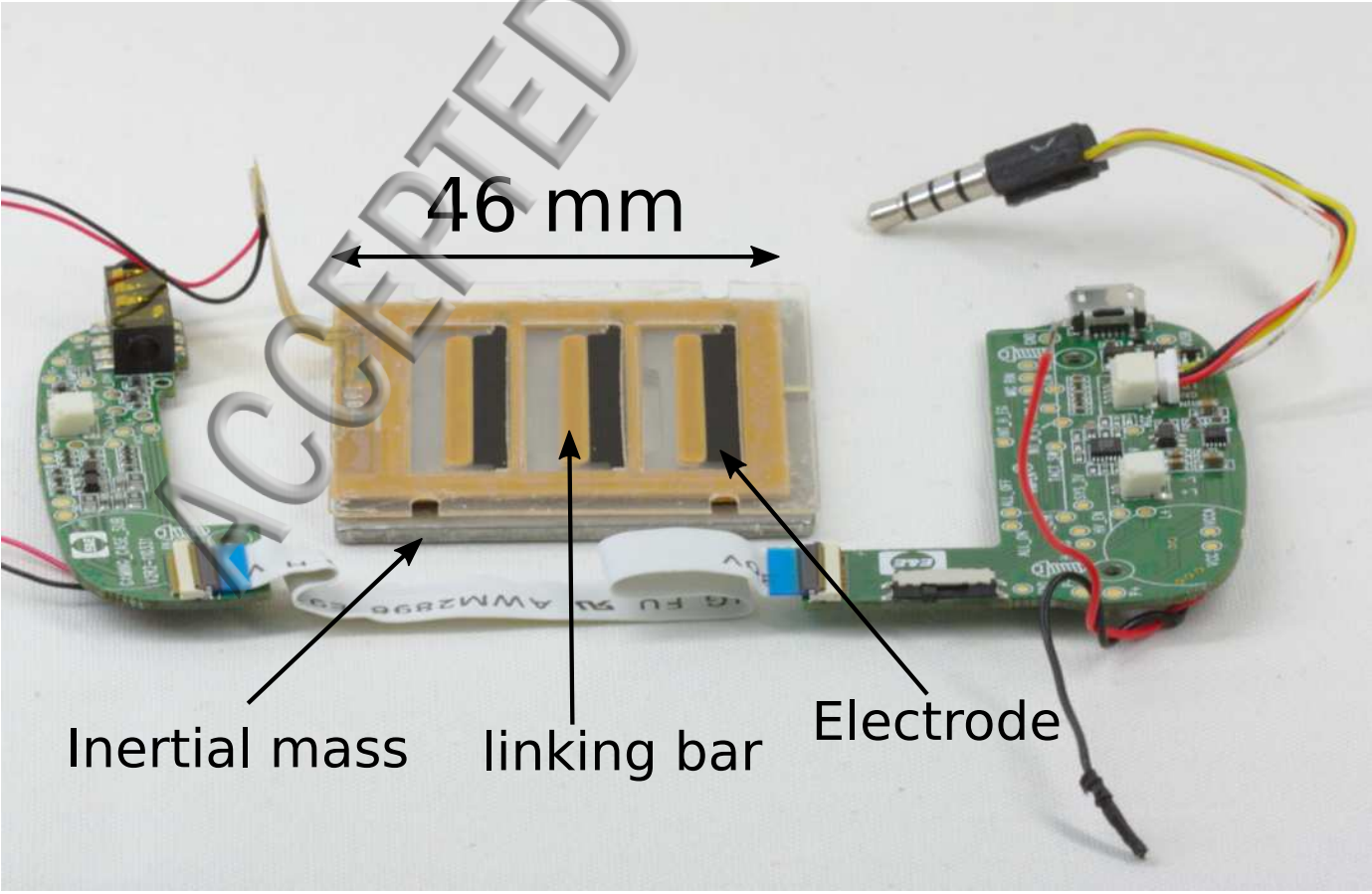
ACCEPTED
46 mm
Inertial mass
linking bar
Electrode

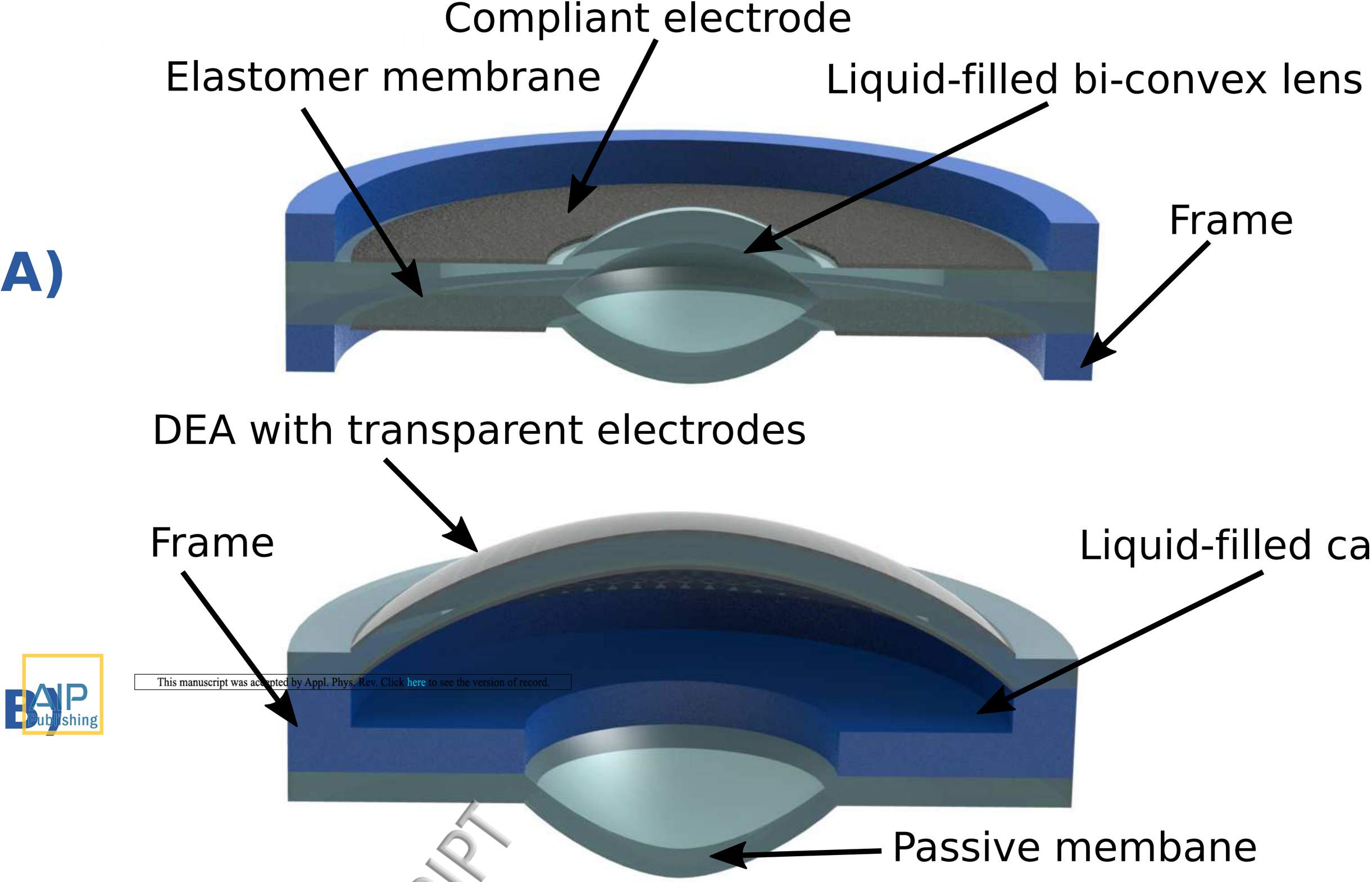

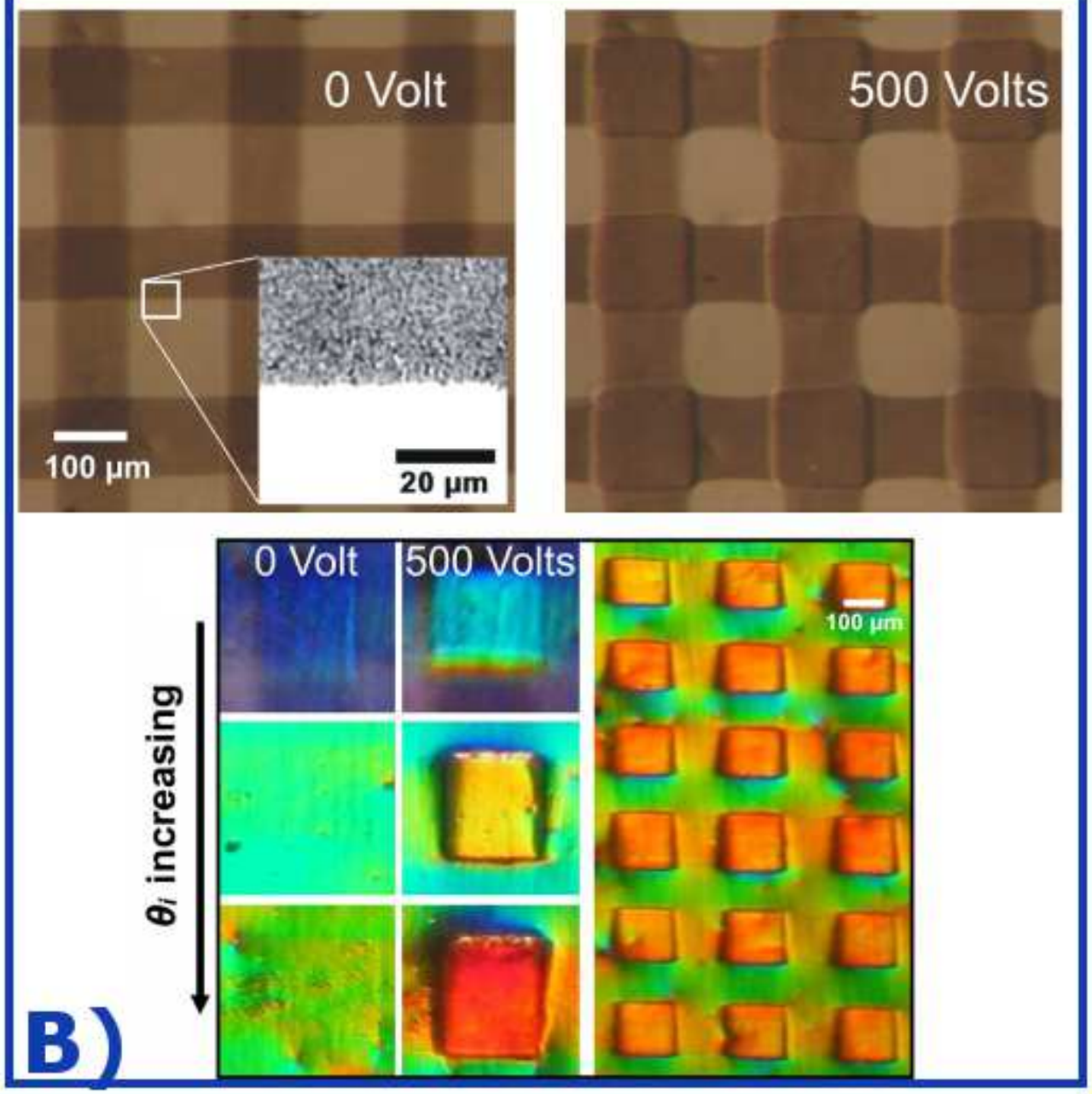

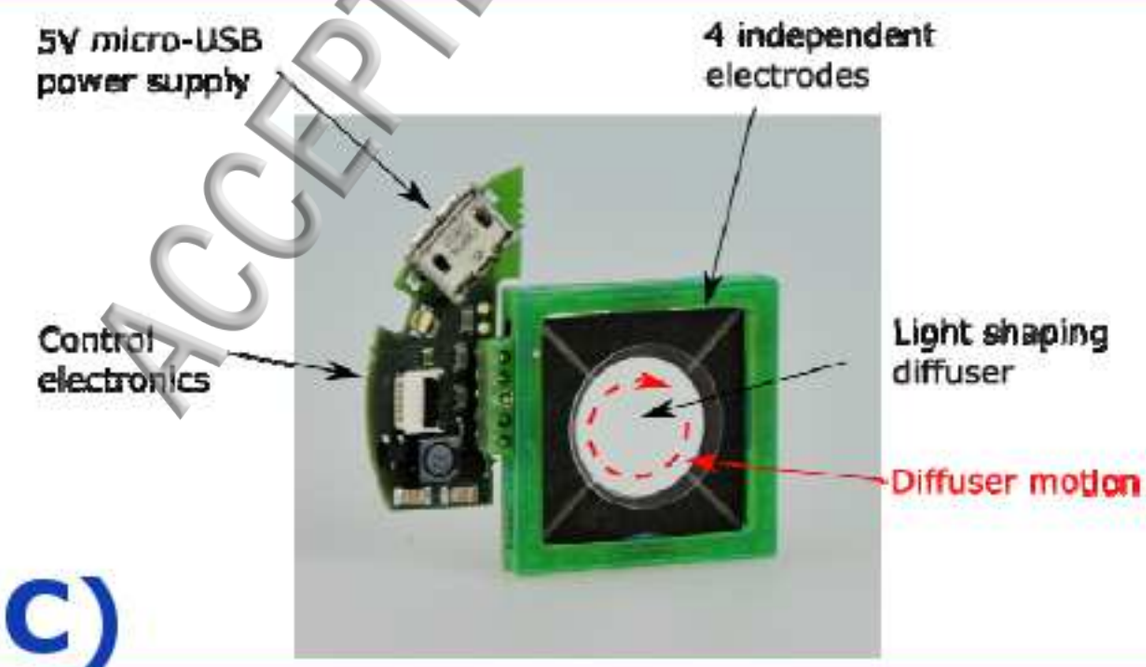

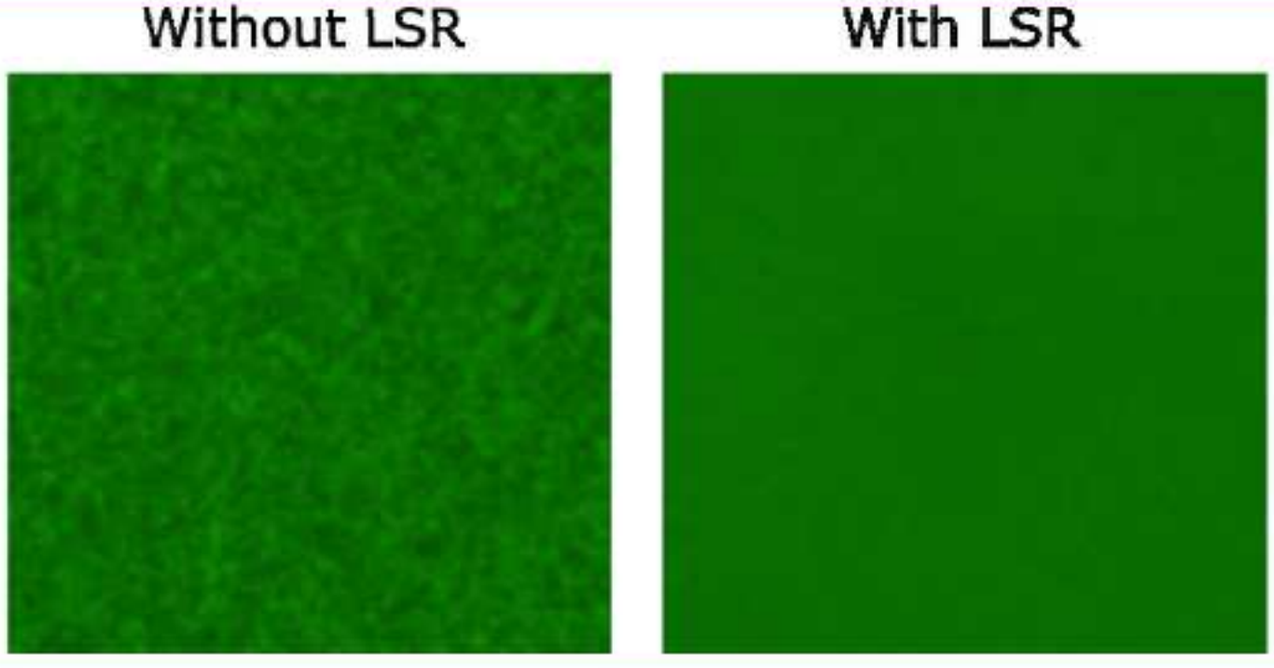

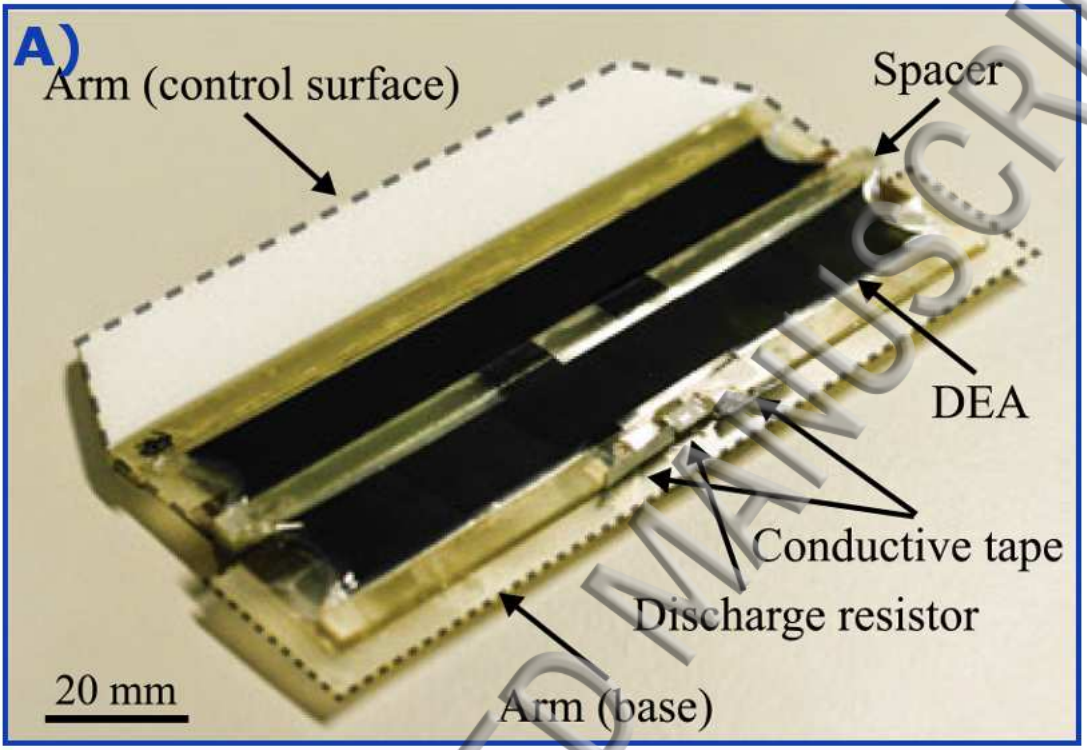

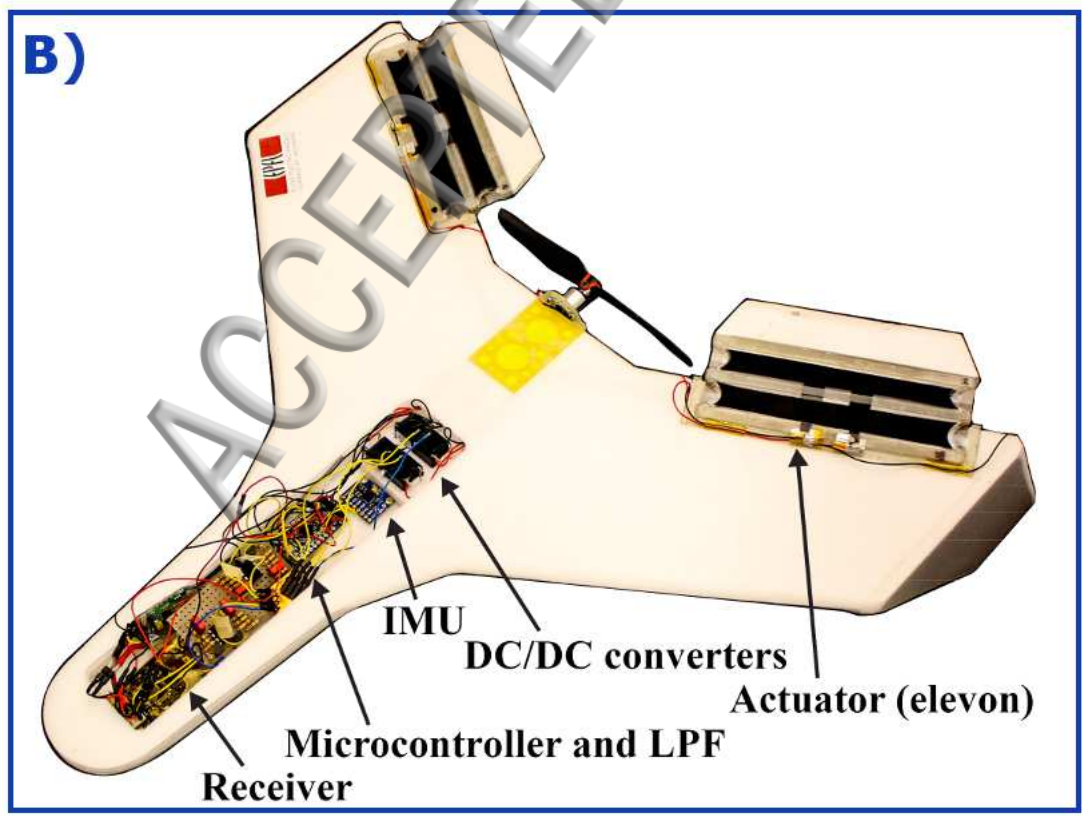

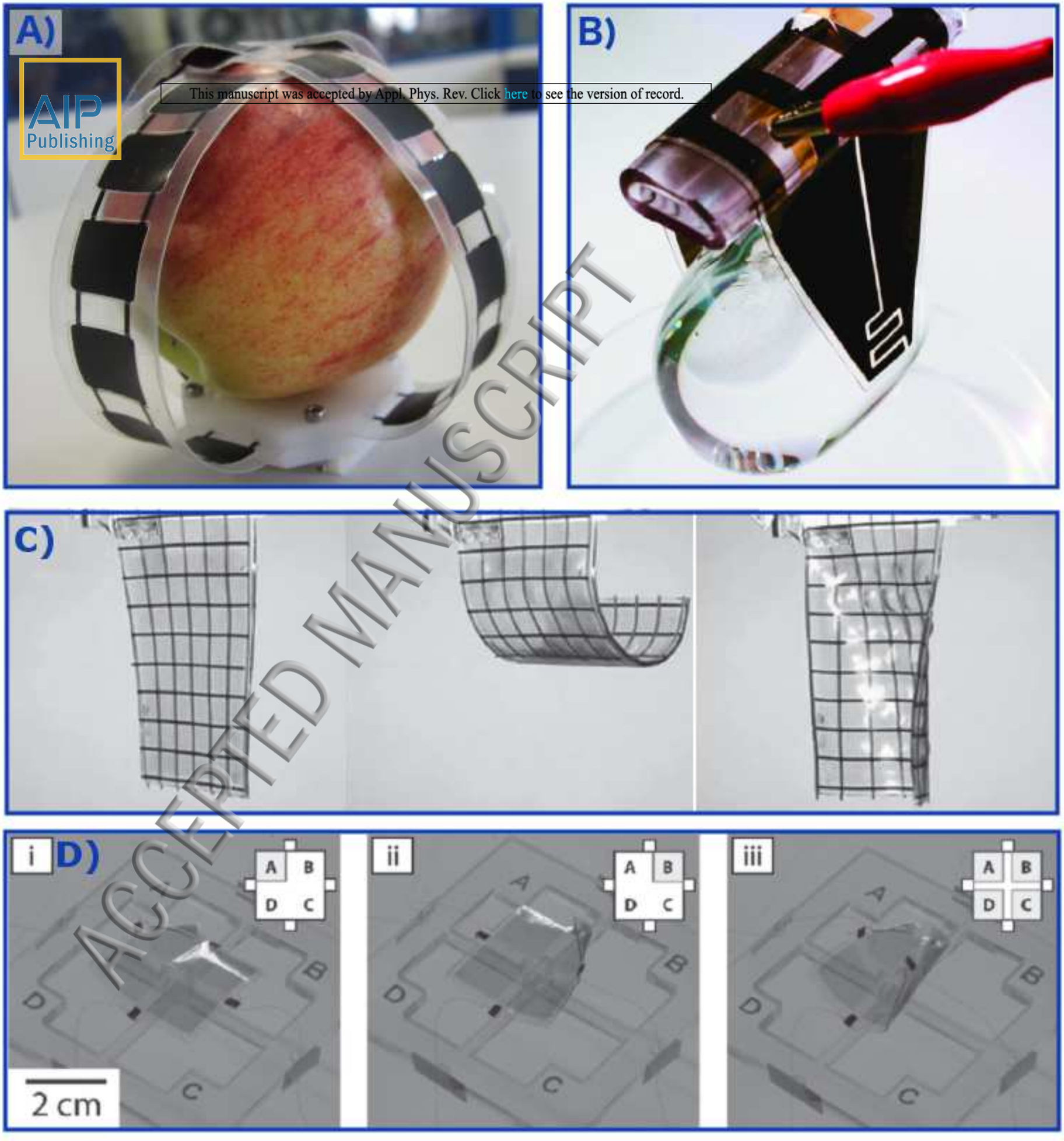

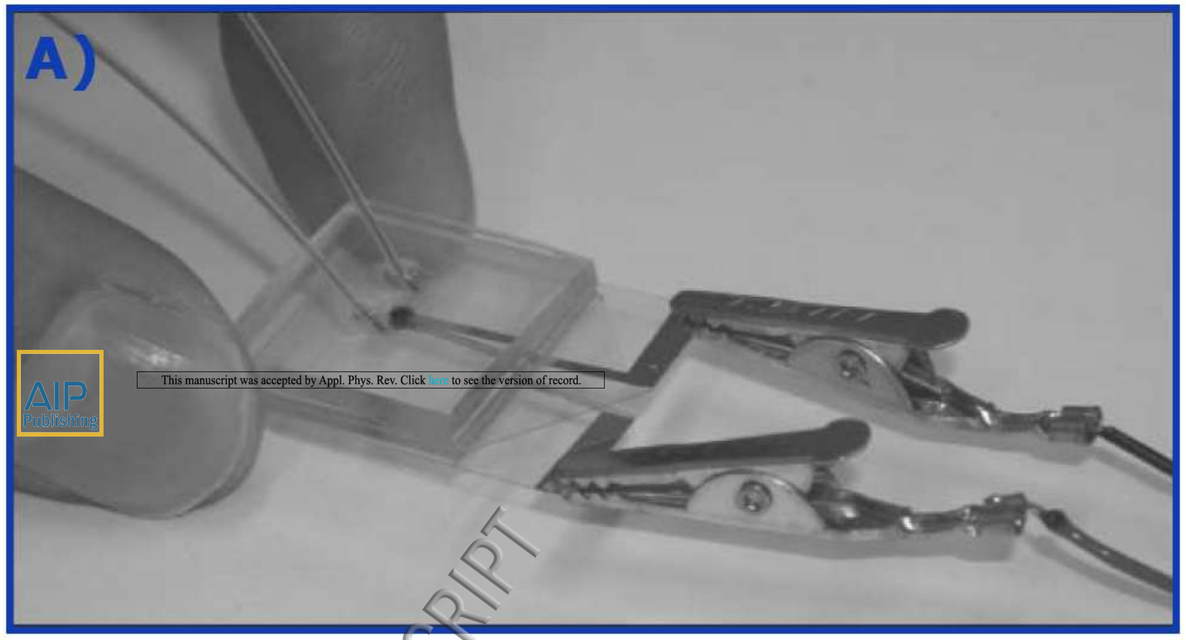

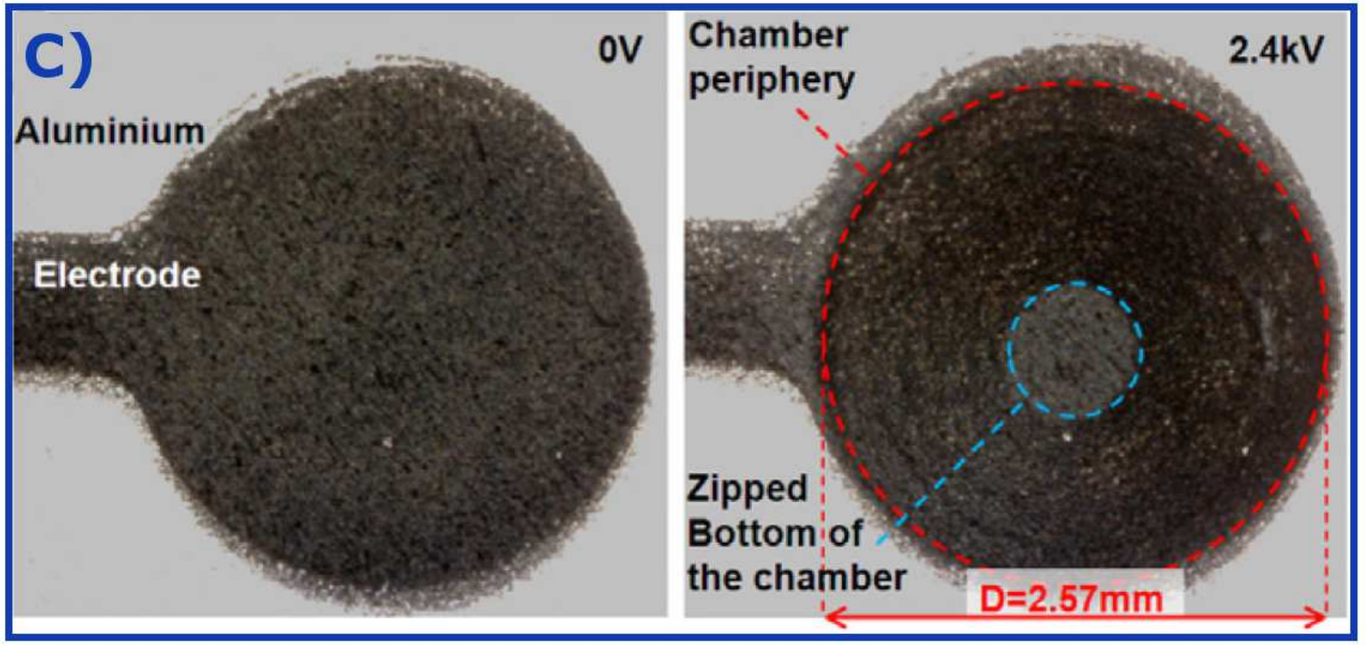

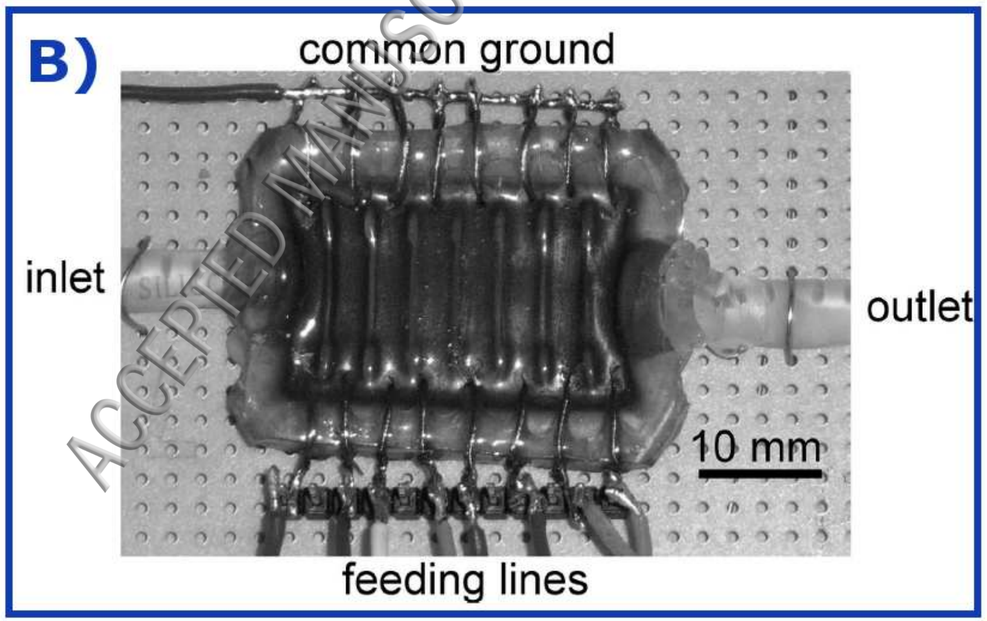

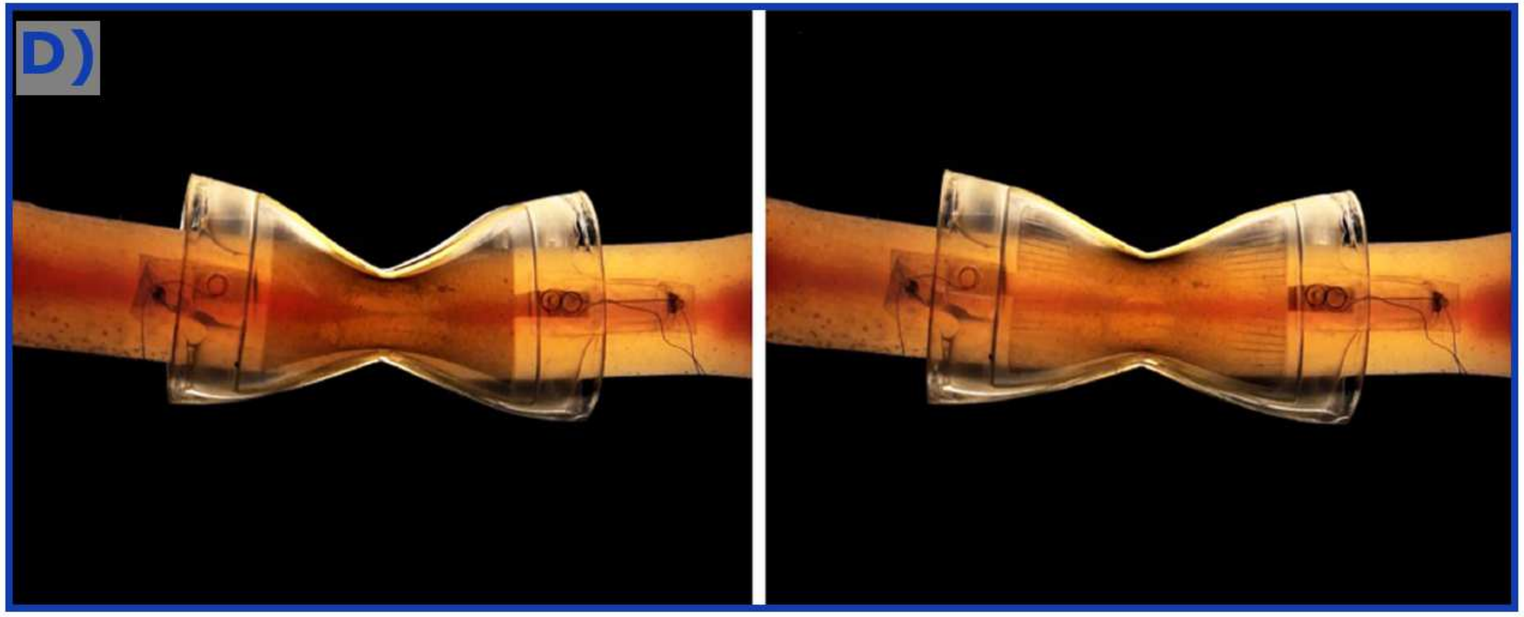

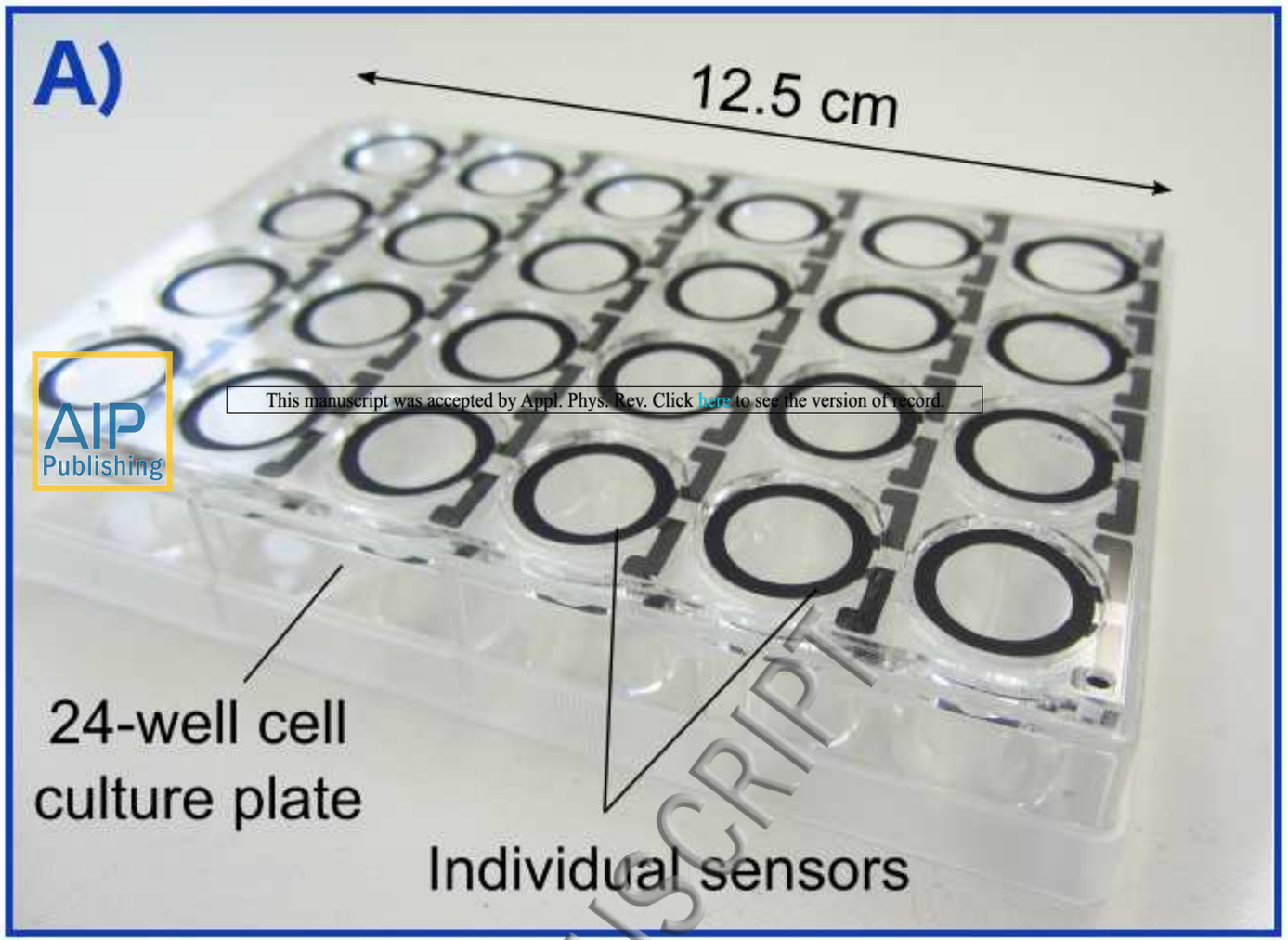

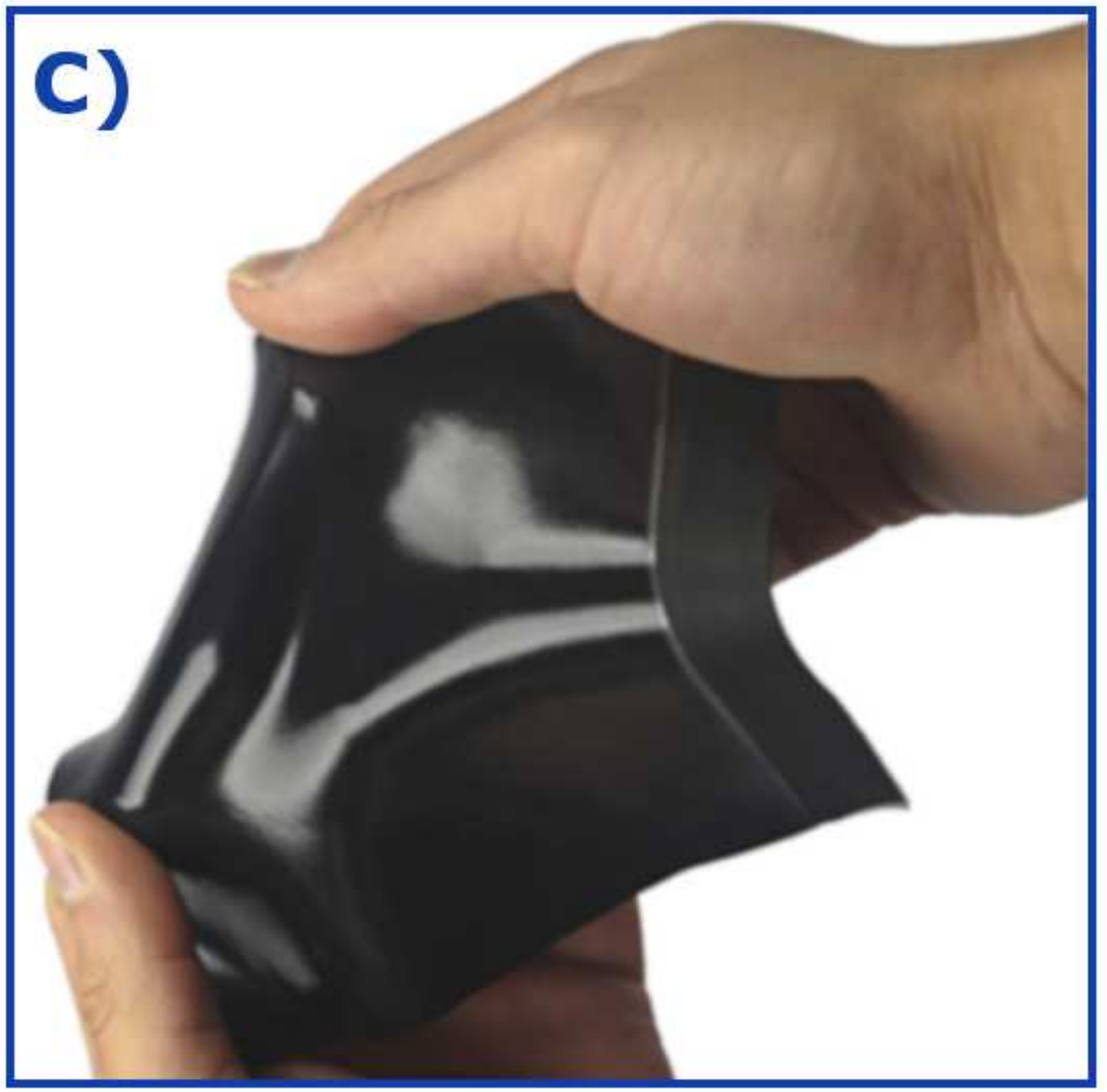

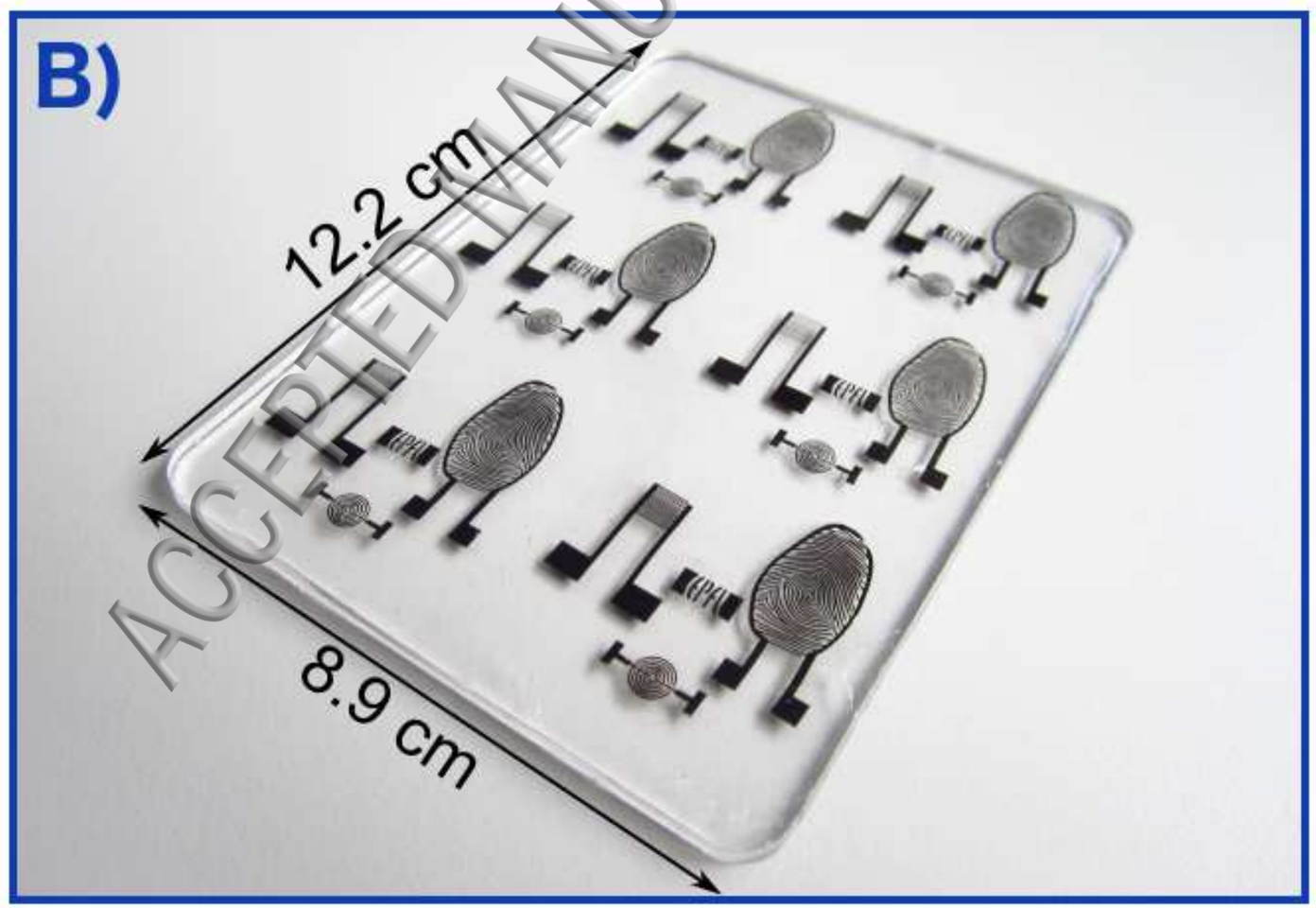

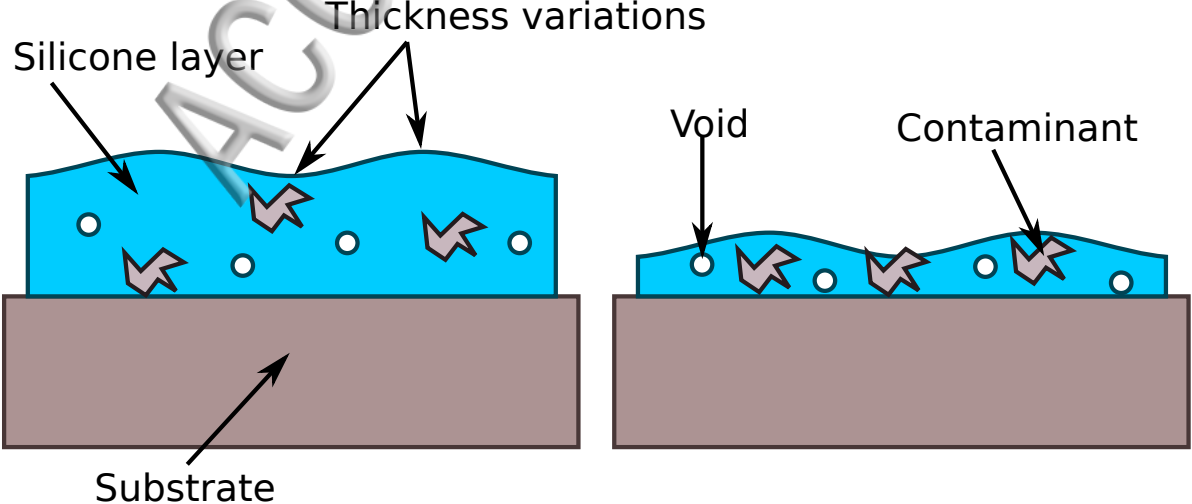
Thickness variations
Silicone layer
Void
Contaminant
Substrate

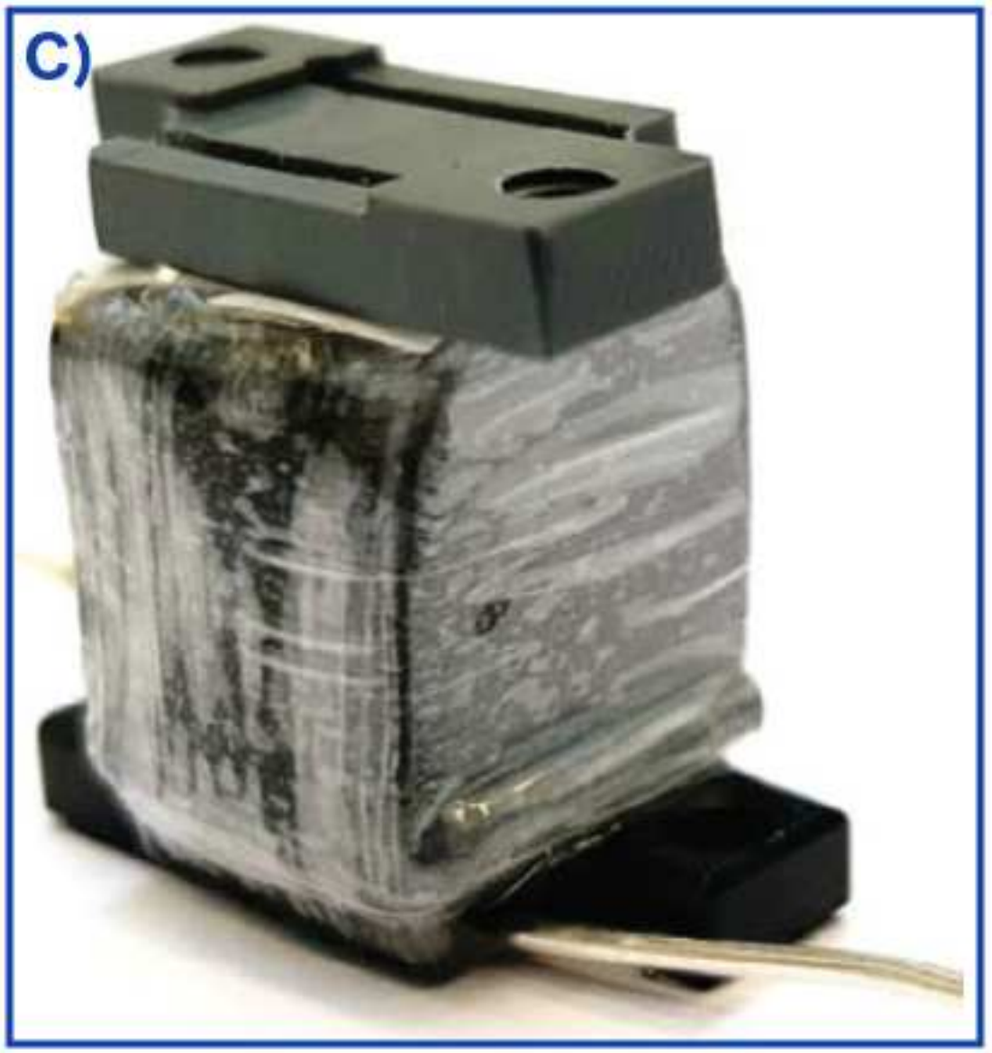

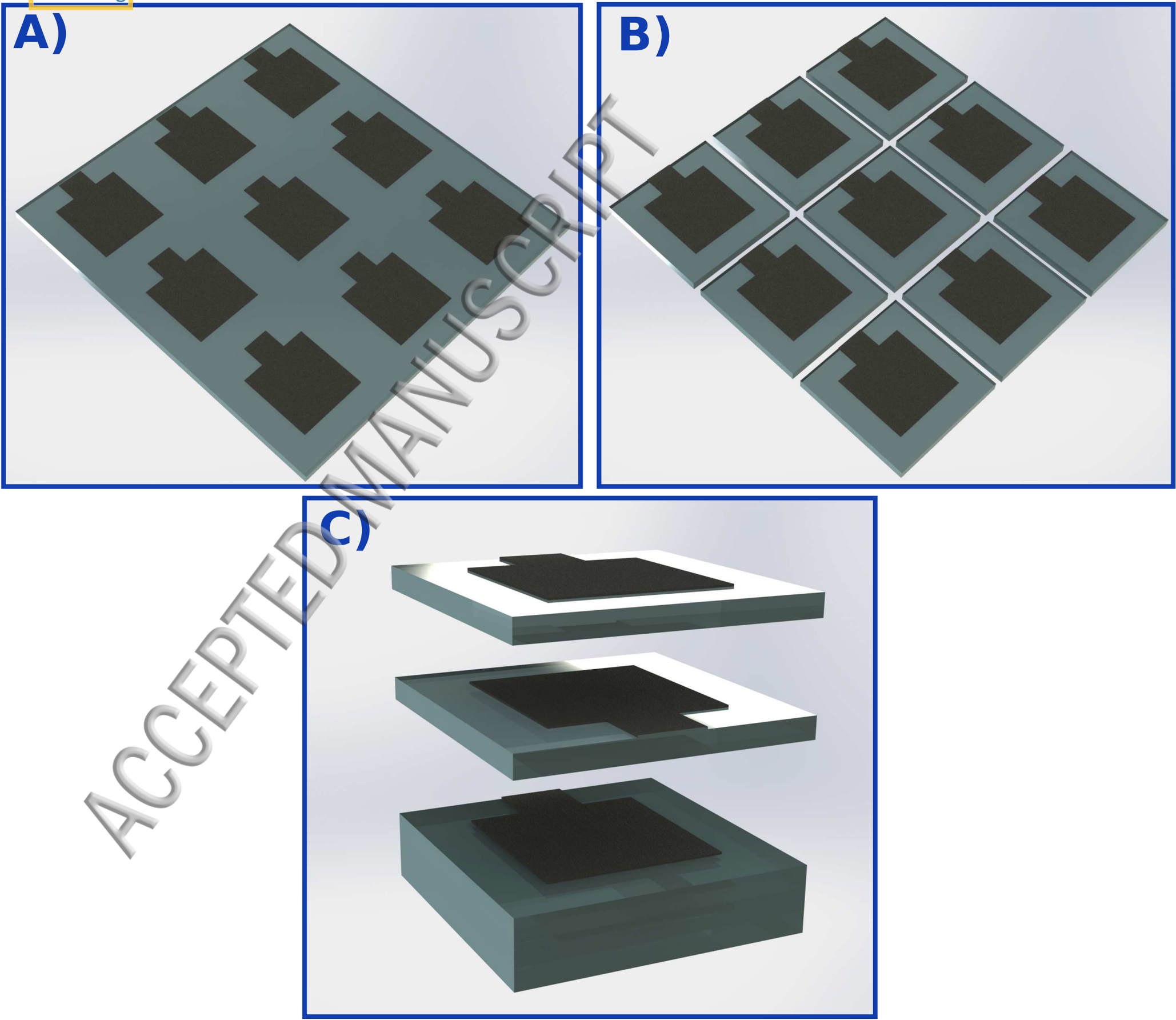

removing the carrier foil

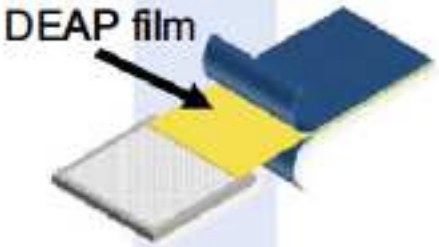

sub-process 1

applying electrodes, folding

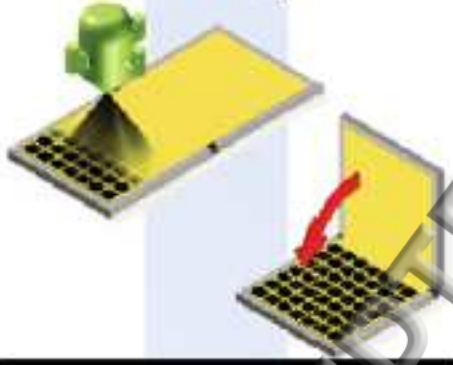

sub-process 2

stacking

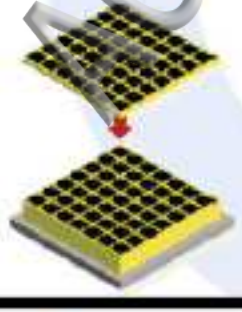

sub-process 3

encapsulating

sub-process 6

contacting

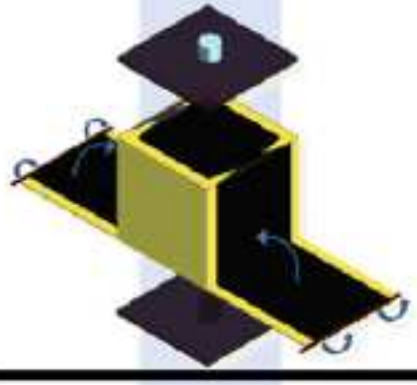

sub-process 5

cutting

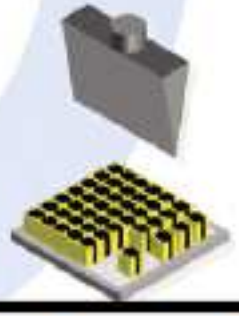

sub-process 4

A)

(1)

DRIE silcion wafer

(2)

Refill with MRTV 9/carbon

(3)

DRIE silicon wafer

(4)

Refill with MRTV 9

(5)

Bond topside-down to handle wafer

(6)

Isotropic silicon etch

(7)

Solvent release

silicon

MRTV 9/carbon

bonding agent

MRTV 9

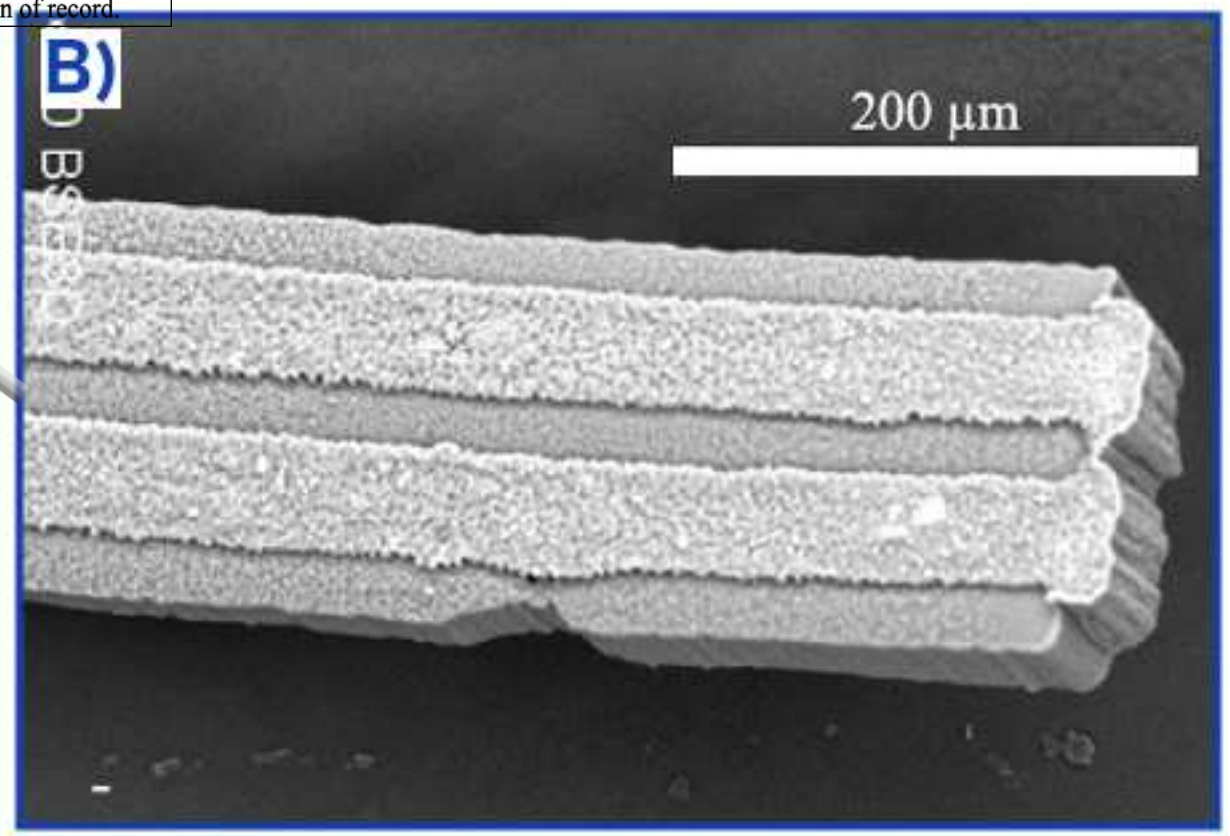

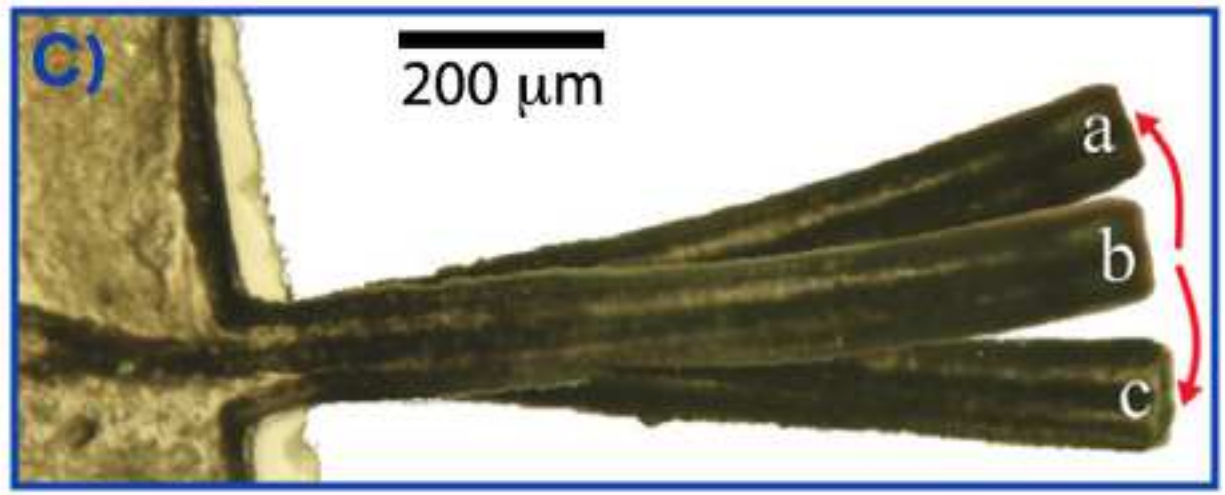

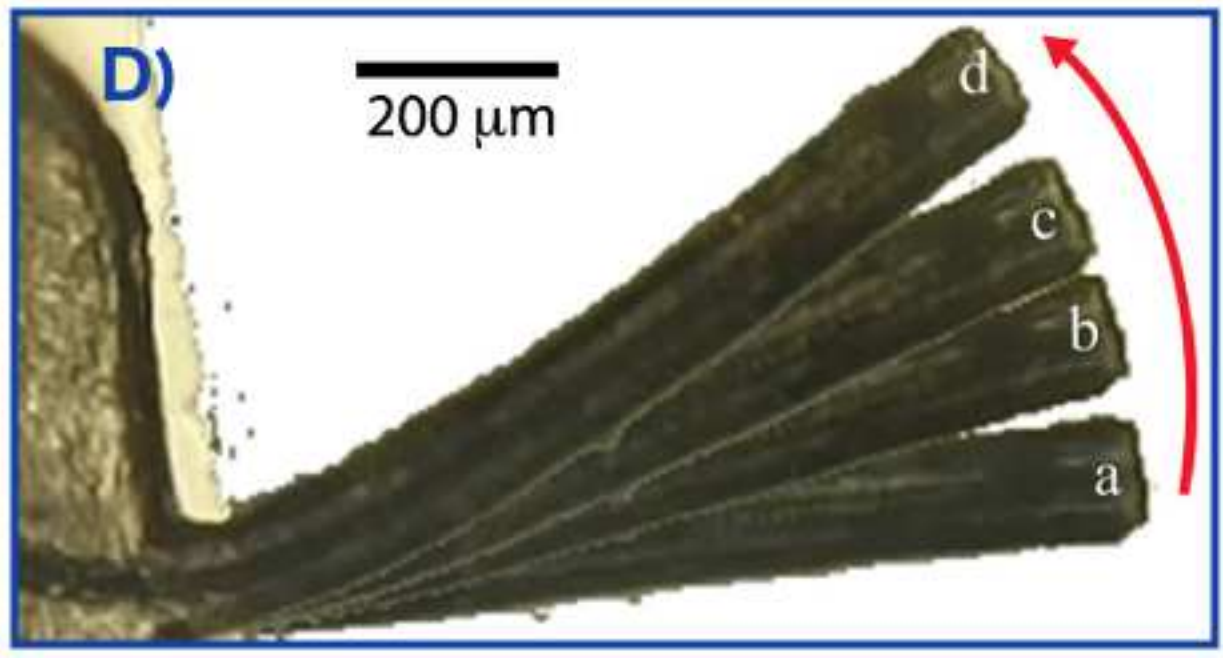

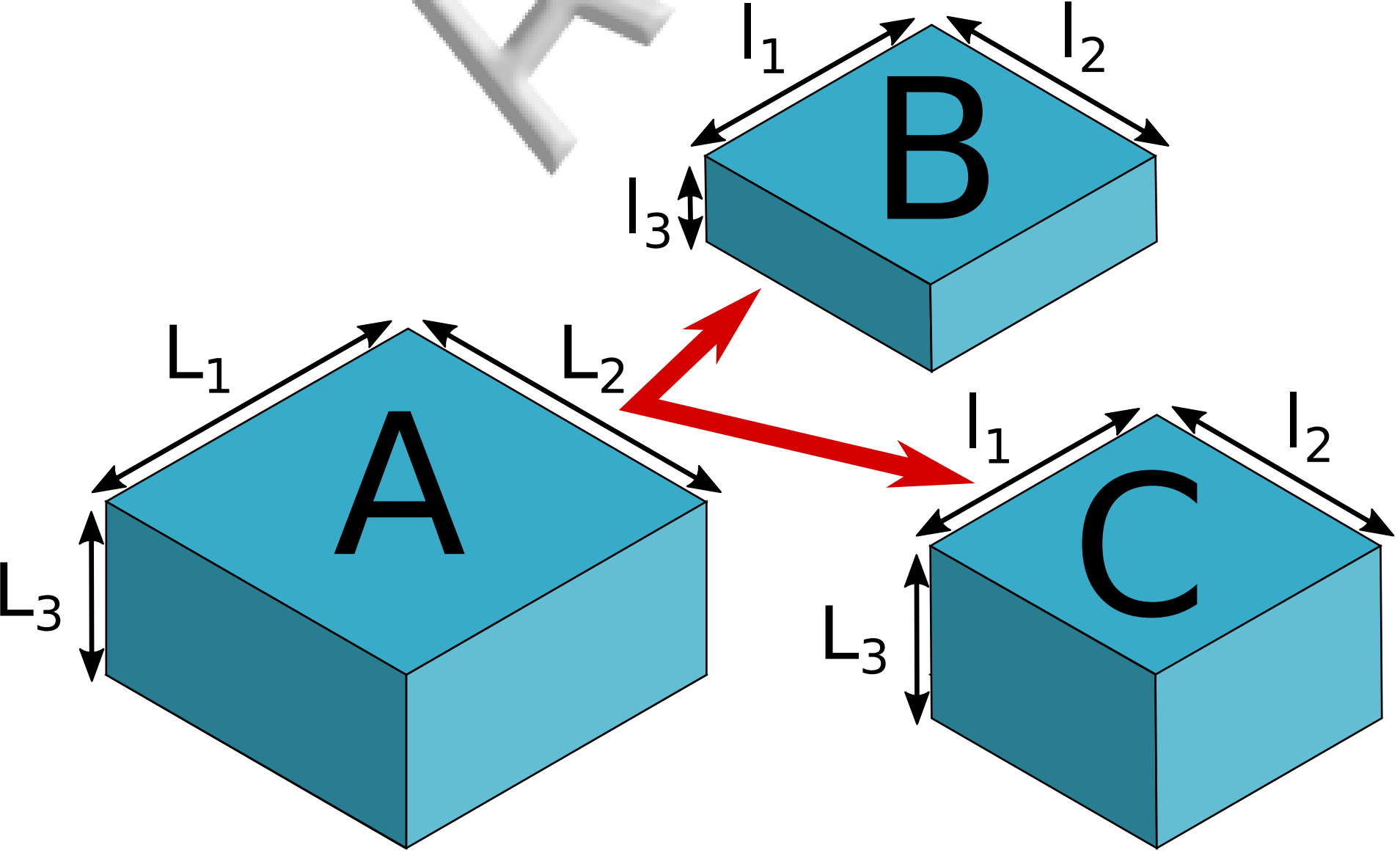
l1
l2
B
l3
L1
L2
A
L3
l1
l2
C
L3

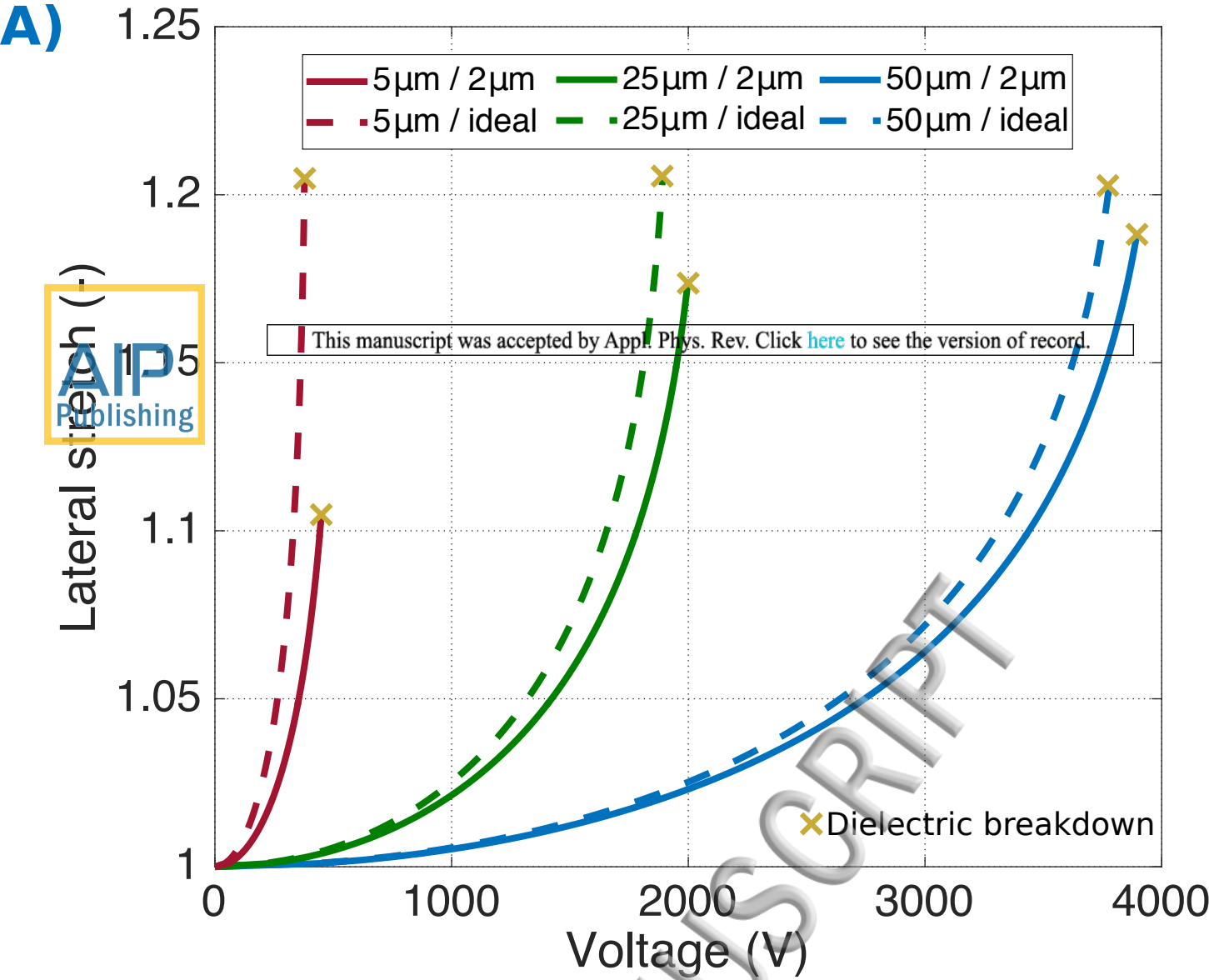

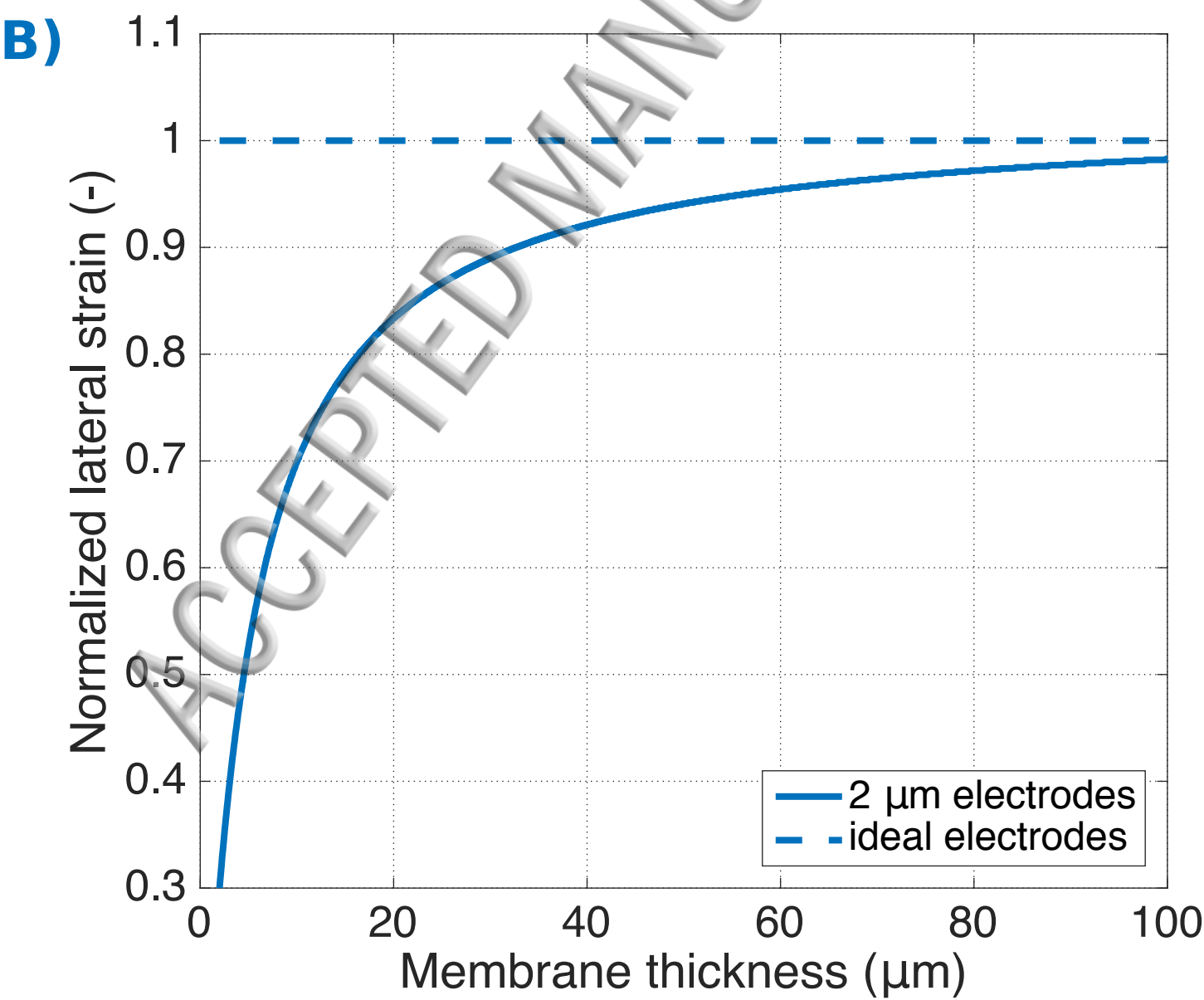

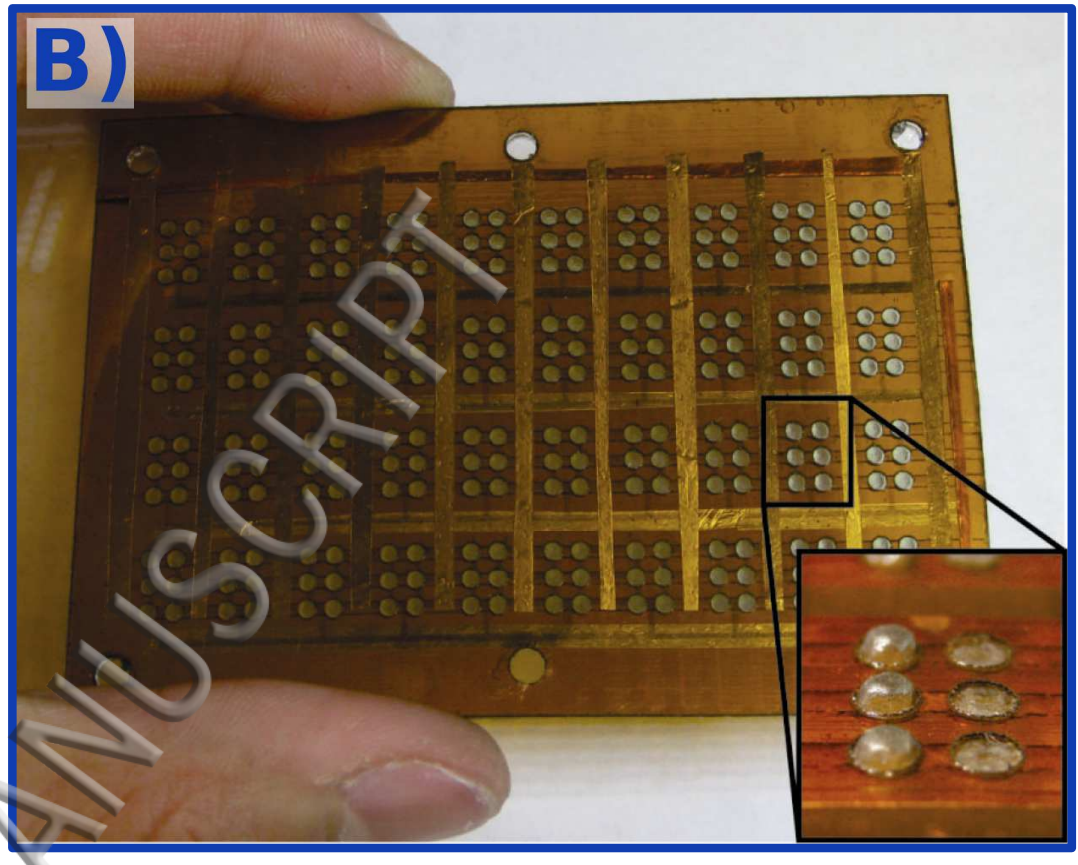

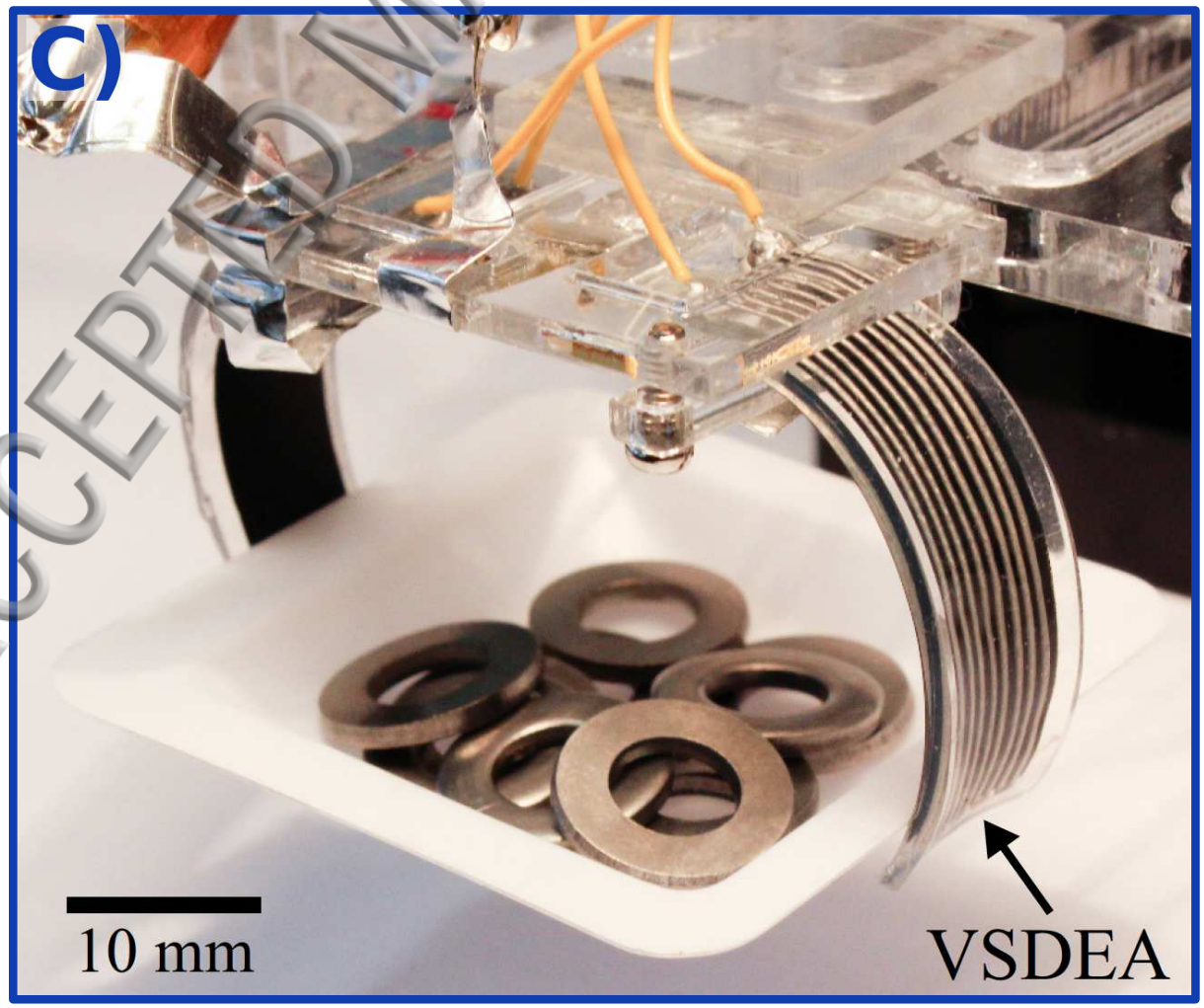

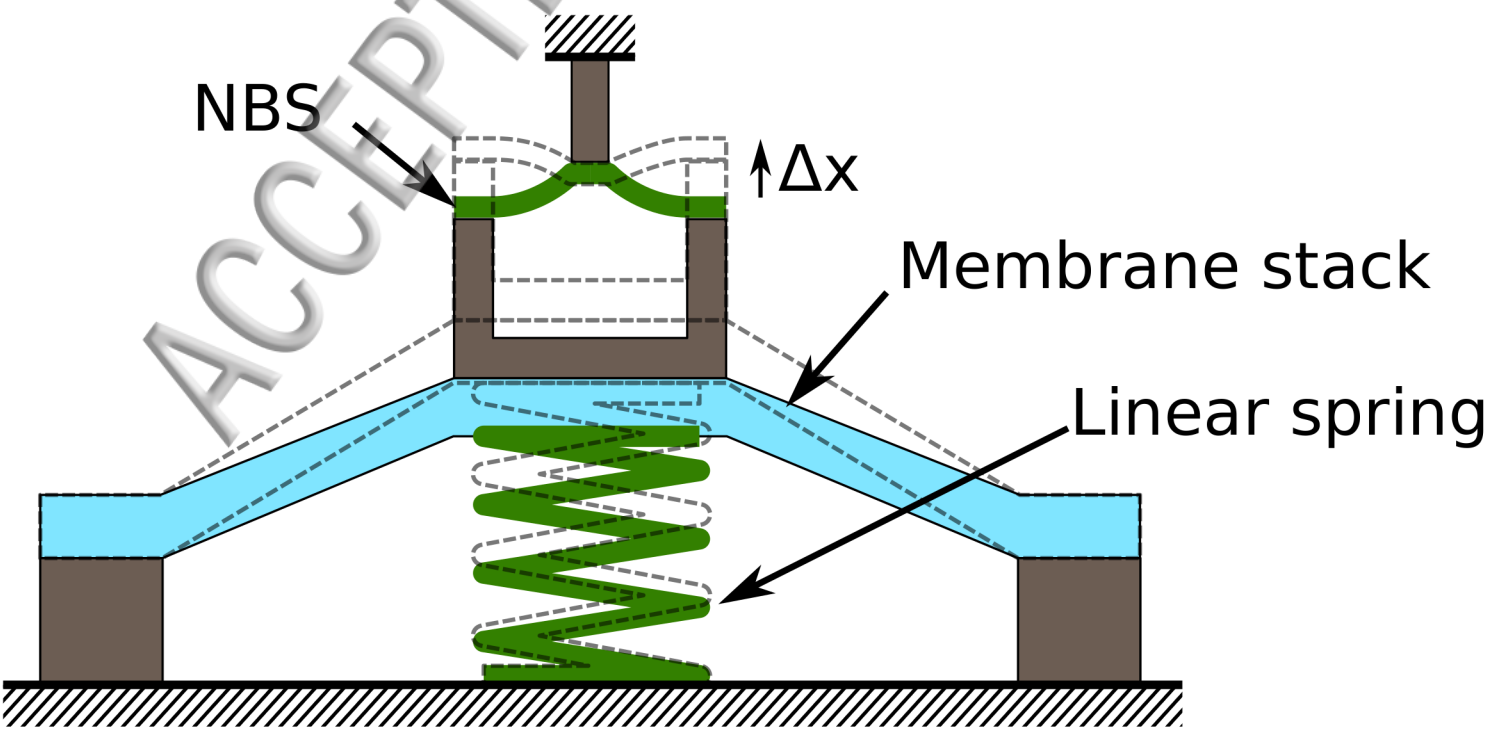
NBS
Δx
Membrane stack
Linear spring